NASA CR-134466

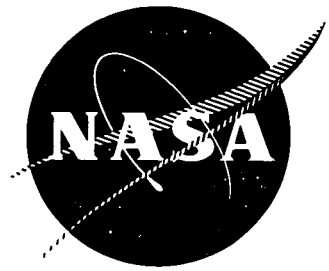

APPLICATION OF DIFFUSION BARRIERS TO THE REFRACTORY FIBERS OF TUNGSTEN, COLUMBIUM, CARBON AND ALUMINUM OXIDE

by F. C. Douglas, E. L. Paradis, and R. D. Veltri

UNITED AIRCRAFT RESEARCH LABORATORY

Prepared for

National Aeronautics and Space Administration

NASA Lewis Research Center
Contract NAS3-15576

1. Report No.	2. Government Accession No.	3. Recipient's Catalog No.
NASA CR-134466		

4. Title and Subtitle	5. Report Date
APPLICATION OF DIFFUSION BARRIERS TO THE REFRACTORY FIBERS OF TUNGSTEN, COLUMBIUM, CARBON AND ALUMINUM OXIDE	September 1973
	6. Performing Organization Code

7. Author(s)	8. Performing Organization Report No.
Frank C. Douglas E. L. Paradis Richard D. Veltri	

9. Performing Organization Name and Address	10. Work Unit No.
United Aircraft Research Laboratories East Hartford Connecticut 06108	
	11. Contract or Grant No. NAS 3-15576

12. Sponsoring Agency Name and Address	13. Type of Report and Period Covered
NATIONAL AERONAUTICS AND SPACE ADMINISTRATION Washington, D. C. 20546	Contractor Report May 1972 to June 1973
	14. Sponsoring Agency Code

15. Supplementary Notes

Project Manager, Leonard J. Westfall
NASA Lewis Research Center, Cleveland, Ohio

16. Abstract

A radio-frequency powered ion-plating system was used to plate protective layers of refractory oxides and carbide onto high strength fiber substrates. Subsequent overplating of these combinations with nickel and titanium was made to determine the effectiveness of such barrier layers in preventing diffusion of the overcoat metal into the fibers with consequent loss of fiber strength.

Four substrates, five doatings, and two metal matrix materials were employed for a total of forty material combinations. The substrates were tungsten, niobium, NASA-Hough carbon, and Tyco sapphire The diffusion-barrier coatings were aluminum oxide, yttrium oxide, titanium carbide, tungsten carbide with 14% cobalt addition, and zirconium carbide. The metal matrix materials were IN 600 nickel and Ti 6/4 titanium.

The results of this survey of barrier coatings are summarized as follows: Ion-plating can produce coatings of sufficient adherence and density to act as diffusion barriers against nickel and titanium for the fibers tested. Barriers for protecting tungsten from nickel are tungsten carbide, titanium carbide, aluminum oxide, and yttrium oxide; protection against titanium is afforded by aluminum oxide and titanium carbide.

Barriers for protecting niobium from nickel are yttrium oxide, zirconium carbide, aluminum oxide, titanium carbide, and tungsten carbide; protection against titanium is poor, the best being given by titanium carbide and tungsten carbide.

Barrier layers for protecting sapphire fibers from nickel are tungsten carbide, and titanium carbide; protection against titanium is given by zirconium carbide and yttrium oxide. Barriers for protecting NASA-Hough carbon against nickel are aluminum oxide and zirconium carbide; protection against titanium is not given. Adhesion of the coatings to all substrates was good except for the NASA-Hough carbon, where flaking off of the oxide coatings in particular was observed.

17. Key Words (Suggested by Author(s))	18. Distribution Statement
Diffusion Barriers, Ion Plating, Refractory Oxide Coating, Refractory Carbide Coatings, Metal Matrix	Unclassified - unlimited

19. Security Classif. (of this report)	20. Security Classif. (of this page)	21. No. of Pages	22. Price*
Unclassified	Unclassified	60	$3.00

*For sale by the National Technical Information Service, Springfield, Virginia 22151

Page Intentionally Left Blank

TABLE OF CONTENTS

LIST OF FIGURES

LIST OF FIGURES (Cont'd)

LIST OF TABLES

SUMMARY

A radio-frequency powered ion-plating system was used to plate protective layers of refractory oxides and carbides onto high strength fiber substrates. Subsequent overplating of these combinations with nickel and titanium was made to determine the effectiveness of such barrier layers in preventing diffusion of the overcoat metal into the fibers with consequent loss of fiber strength.

Four substrates, five coatings, and two metal matrix materials were employed for a total of forty material combinations. The substrates were tungsten, niobium, NASA-Hough carbon, and Tyco sapphire, The diffusion-barrier coatings were aluminum oxide, yttrium oxide, titanium carbide, tungsten carbide with 14% cobalt addition, and zirconium carbide. These were ion-plated to a thickness of the order of two micrometers onto the fibers. The metal matrix materials were IN 600 nickel and Ti 6/4 titanium. These metals were ion-plated onto the fiber/barrier combinations to a thickness of the order of 200 micrometers (0.2 millimeters).

Tensile fracture tests were performed on the as-received fiber substrates, on the fiber/barrier and fiber/matrix combinations, and on the fiber/barrier/matrix combinations. These tensile tests were performed to study the possible loss of strength due to the plating process and/or the thermal exposures to which the systems of fiber/coatings were subjected. In addition, the process of ion-plating itself was under study to determine the adherence of the coatings and their effects on the fibers.

The scanning electron microscope (SEM) was used as an analytical tool to provide visual evidence for evaluation of coating adherence and mode of tensile fracture. Metallographically prepared cross-sections were made of selected fiber/coating combinations and etched to determine if metal matrix diffusion through the barrier layers could be detected by differential etching. In cases where such etching studies appeared to indicate a reaction area, the electron microprobe was employed to determine element distribution.

Additional tests of performance were tensile tests of fiber/barrier/matrix combinations at 860°C. A nine-minute exposure prior to tensile fracture was used in these tests.

The results of this survey of barrier coatings may be summarized as follows: Ion-plating can produce coatings of sufficient adherence and density to act as diffusion barriers against nickel and titanium for the fibers tested. Barriers for protecting tungsten from nickel are tungsten carbide, titanium carbide, aluminum oxide, and yttrium oxide; protection against titanium is afforded by aluminum oxide and titanium carbide.

Barriers for protecting niobium from nickel are yttrium oxide, zirconium carbide, aluminum oxide, titanium carbide, and tungsten carbide; protection against titanium is poor, the best being given by titanium carbide and tungsten carbide.

Barrier layers for protecting sapphire fibers from nickel are tungsten carbide, and titanium carbide; protection against titanium is given by zirconium carbide and yttrium oxide.

Barriers for protecting NASA-Hough carbon against nickel are aluminum oxide and zirconium carbide; protection against titanium is not given.

Adhesion of the coatings to all substrates was good except for the NASA-Hough carbon, where flaking off of the oxide coatings in particular was observed.

Recommendations for further studies of diffusion barrier coatings on high strength fibers include yttrium and aluminum oxides and titanium, tungsten, and zirconium carbides as protectors for tungsten, niobium, and sapphire fibers.

INTRODUCTION

Fiber-strengthened composite materials have been extensively investigated during the past few years because their properties can be tailored to satisfy the requirements of particular applications. A major problem area in the fabrication and use of metal matrix composites is that of reactions between the fiber and the matrix during the fabrication of the composite, and/or during the use of such composites at elevated temperatures. In particular, fibers for use in nickel alloy matrix composites which can withstand temperatures up to 1200 deg. C for 1000 hours or for incorporation into titanium matrix composites whose fabrication temperatures exceed 870 deg. C are not available. The objective of this program was to evaluate materials for diffusion barriers on high strength fibers resulting in non-reactive fibers with sufficient strength for metal matrix reinforcement.

The approach investigated in this work is that of finding a coating for a high strength fiber which, when applied by the ion plating technique, forms a protective diffusion barrier between the fiber and the metal matrix material which it is used to strengthen. Tensile testing of the fiber-barrier-matrix combinations was used to evaluate both the effects of the ion-plating process itself and the effects of thermal exposures on the strengths of the combinations. Scanning electron microscope examinations of tensile fracture surfaces were used in conjunction with the tensile test results to evaluate the strength values obtained in terms of effects which are displayed topographically, such as flaw-initiated fractures. Electron microprobe analyses, along with metallographic preparations and etching, were used to search for significant diffusion reactions. Hot tensile tests were used to examine the effects of temperature on the strength of the coated fibers at the expected service temperature.

The ion-plating of the fibers was carried out using a cylindrical target 38.1 cm long, 6.35 cm OD, and 5.08 cm ID. Ions for target bombardment were generated with 13.7 MHz RF energy; the ions and atoms of the target were plated onto fibers which were suspended on a grounded stainless steel rod along the axis of the cylindrical target.

Fiber materials used in this work were tungsten, niobium, NASA-Hough carbon, and Tyco single-crystal sapphire fiber. The materials used as barrier layers were aluminum oxide, yttrium oxide, titanium-carbide, zirconium carbide, and tungsten carbide with 14% cobalt. The matrix materials used were nickel (IN600) and titanium (Ti-6/4).

EXPERIMENTAL PROCEDURE

Ion Plating: Apparatus and Operation

The ion plating apparatus used in the present work was designed and developed at the United Aircraft Research Laboratories as a research tool for the deposition of a variety of materials in thin film form. For the present work, right circular cylindrical targets were used from which the required material was removed from the inner wall of the cylinder and deposited onto fiber substrates which were suspended along the axis of the target.

The mechanisms and benefits of the deposition of thin films by ion plating have been discussed in detail by several authors (Refs. 1, 2, 3). To produce good quality films, a chamber is required which can be evacuated to about 10^{-6} torr, then partially backfilled with an inert gas. The plating source must be capable of supplying the plating material in a vapor form such as an evaporation source or a sputtering target. There must be a means of initiating a glow discharge in the low pressure gas in the region of the substrate. Finally there must be an electrical circuit which can maintain a negative bias on the substrate.

Before the plating source is energized, the gas discharge (plasma) is struck and the bias is applied to the substrate. In this way the substrate is sputtered clean prior to film deposition. The plating source is then energized with the bias still applied to the substrate and deposition takes place on the atomically clean substrate surface. The fact that the substrate can be so well cleaned just prior to depostion is the aspect of ion plating which is principally responsible for producing outstandingly adherent films.

The negative bias is maintained throughout the deposition process, although generally at a reduced potential. This bias during deposition aids in promoting good film adherence by sputtering away loosely bound contaminants and repelling negatively charged contaminants. The added energy imparted to the deposited species by the bombarding ions of the plasma serves to enhance surface migration of the deposited atoms resulting in further improvement of film quality.

Because the deposition takes place at gas pressures in the millitorr range, considerable scattering of the depositing source atoms takes place with the gas molecules. This scattering accounts primarily for the plating of surfaces out of the line of sight of the source.

For the coating of fibers, a cylindrical geometry capable of inward sputtering was used. This arrangement has the advantage that it promotes uniform deposition because of the similar geometry of source and substrate. Furthermore,

enhanced deposition rates result because of the concentration effect as the deposit travels inward toward the axis. Finally, this geometry conserves source material because, except for small losses at the ends of the cylinder, the source material that is not intercepted by the substrate and holder is returned to another part of the target to be resputtered.

Several versions of cylindrical cathodes have been developed at the UARL for RF sputtering. The modification that was used to coat fibers for this program is illustrated in Fig. 1. The targets used in this program were right circular cylindrical shells 38.1 cm (15 inches) long, with a 6.35 cm (2.5 inches) outside diameter and a 0.3175 to 0.635 cm (.125 to .250 inches) thick wall. The ion plating targets used in this work were hot-pressed cylinders which were obtained from the vendors listed in Table I. Other targets were obtained but were damaged in some way which precluded their use. This occurred with both the aluminum oxide and yttrium oxide targets, for which replacements were obtained, and with titanium diboride, which was not replaced during the time span of the contract. A target of magnesium zirconate was planned for evaluation, but could not be obtained.

The metal matrix material was IN600 nickel purchased from Whitehead Metals, and the Ti-6/4 titanium was obtained as a hot-forged round bar from Pratt and Whitney Aircraft. Both the nickel and the titanium were machined to the cylindrical target shape.

The ceramic targets were metallized on their outside surfaces, then they, as well as the metal targets were indium soldered directly to the inner wall of a copper cathode.

The copper cathode is double walled so that water can be circulated to keep the target cool to avoid thermal stressing. The cooling water as well as the RF power is fed in through a coaxial tube threaded to the cathode. The cathode is insulated from ground by a pair of ceramic standoffs at each end. A thin walled copper radiation shield surrounds the cathode and power lead. This shield also served to support the windings of a cylindrical electromagnet. The electromagnet serves to increase the plasma density in the vicinity of the target by confining the secondary electrons emitted from the target. Up to a point, an increase in plasma density results in an increase in deposition rate. Further, because they are confined to spend more time in the vicinity of the target, the electrons are somewhat thermalized before reaching the fibers. This results in much less heating of the substrate than there would be otherwise.

The fiber substrates are held in an 8-jaw chuck and suspended parallel to the target axis at a radial distance of 0.635 cm (0.25 inches). A ceramic separator holds them at this radius and prevents the fibers from touching each other. The negative bias is applied to the fibers through an insulated feed through on the end cap. For the deposition of electrically insulating coatings, the bias must be radio frequency energy.

CYLINDRICAL ION PLATING APPARATUS

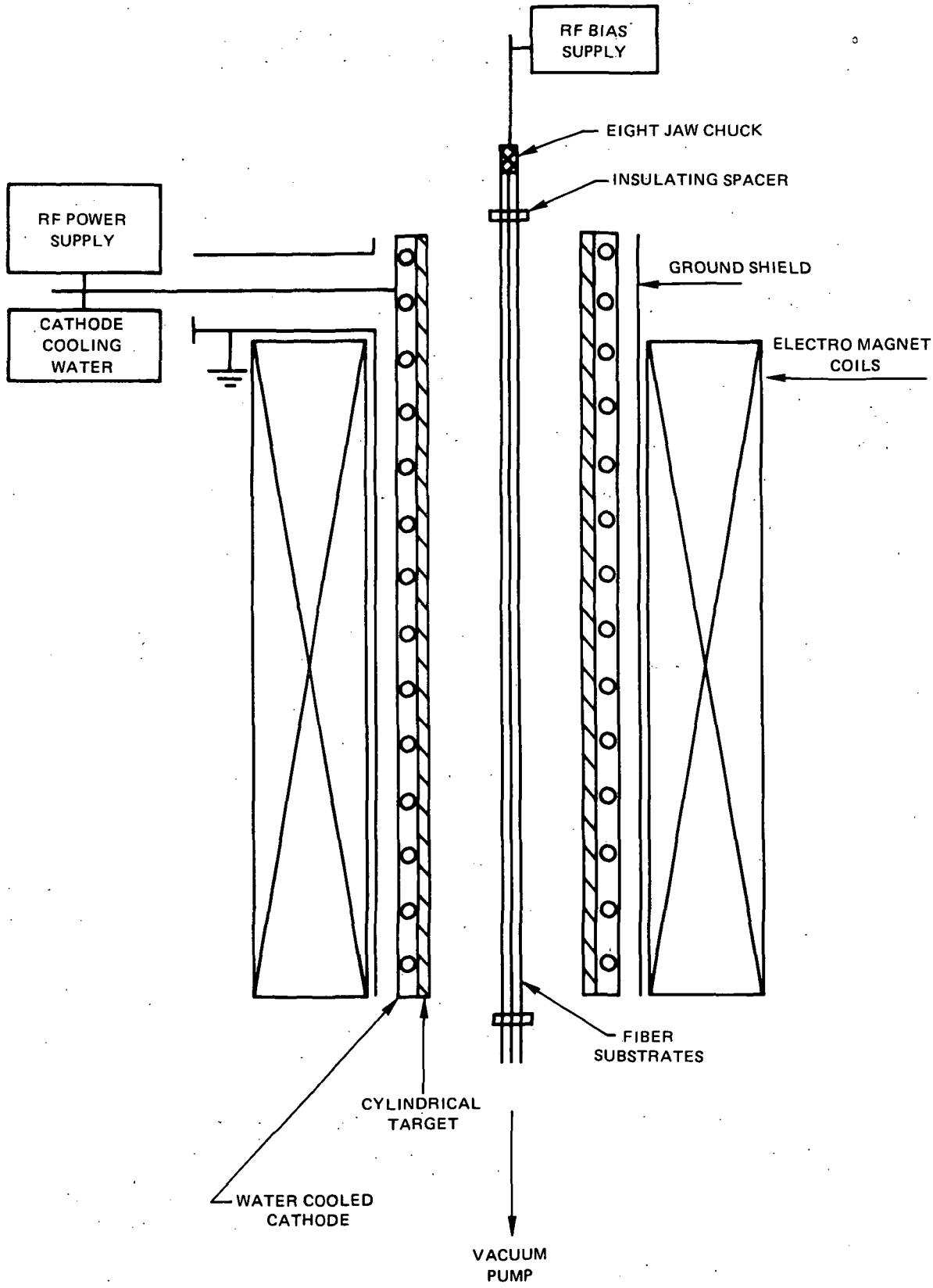

TABLE I

Ion Plating Cylindrical Targets

aluminum oxide	McDanel (1)
yttrium oxide	Haselden (2)
titanium carbide	Cerac (3)
zirconium carbide	Haselden
tungsten carbide + 14% cobalt	Haselden

(1) McDanel, Inc.
Beaver Falls, Pennsylvania

(2) Haselden Co.
San Jose, California

(3) Cerac, Inc.
Menomonee Falls, Wisconsin

The fiber substrates were prepared by cutting lengths about 45.7 cm (18 inches) from the spools of stock provided by NASA. The lengths were mounted in the substrate holder. The entire assembly was then irrigated with MOS grade trichloroethylene, rinsed with MOS grade methanol, and blown dry in a gentle stream of dry nitrogen.

The cylindrical cathode is pumped with a conventional oil diffusion pump backed with a mechanical pump. A liquid-nitrogen-cooled optical baffle is located between the diffusion pump and the cathode. Typically the system is initially pumped down to about 2×10^{-6} torr. The high vacuum valve is then partially closed and 99.999 percent pure argon is admitted through a precision micrometer valve. A dynamic balance is achieved between the inlet gas and the exhaust such that a pressure of 15×10^{-3} torr is maintained in the cathode and 25×10^{-3} torr in the foreline of the diffusion pump.

During a typical run about 100 volts rms RF bias is applied to the fibers and a total of 50 watts is applied to the cathode for the initial 5 minutes. This combination of power inputs allows the fiber to sputter clean while at the same time the target is sputtering only fast enough to avoid being contaminated by what is being removed from the fibers. The sputterant from the fibers is deposited on the substrate holder fixturing. During the next 5 minutes the power input to the target is gradually raised to one-half of the final operating value. This provides a gradual transition from cleaning to coating, to assure that when coating starts, only clean target material is being deposited. The power is then increased to full value and the bias decreased to about 50 volts rms for the remainder of the run.

The duration of the run is directly related to the deposition rate and the total film thickness required. Deposition rates were determined for all materials deposited in this program and a summary is presented in Table II.

All of the rates listed in Table II are for an input power density of 1.58 watts per cm^2. This power density is equivalent to a total input power of 1000 watts. All materials were deposited at this input power with the exception of Al_2O_3 which was deposited at 1600 watts and nickel and titanium which were deposited at 2000 watts. Power inputs were limited to 1000 watts because early in the program it was found that the Y_2O_3 target would not sustain electrical stresses greater than 1.58 watts per cm^2 without failure. In order to avoid delays in the program due to replacing broken targets resulting from excess electrical stresses, it was decided to limit the power input on all of the ceramic targets to 1000 watts.

The deposition profile as a function of position along the axis was also determined. It is presented in Fig. 2. Note that for the 30.5 cm (12 inch) long interval between detectors at 10.2 cm (4 inches) and 40.6 cm (16 inches) that the deposition is reasonably uniform. The variation of about $\pm$ 10 percent from the

TABLE II

Deposition Rates in Cylindrical Cathode

Power Input 1.58 watts/cm^2

Material	Rate Å/min
Al_2O_3	85
Y_2O_3	40
TiC	200
ZrC	160
WC + 14% Co	440
IN600-Ni	750
Ti-6Al-4V	800

FIG. 2

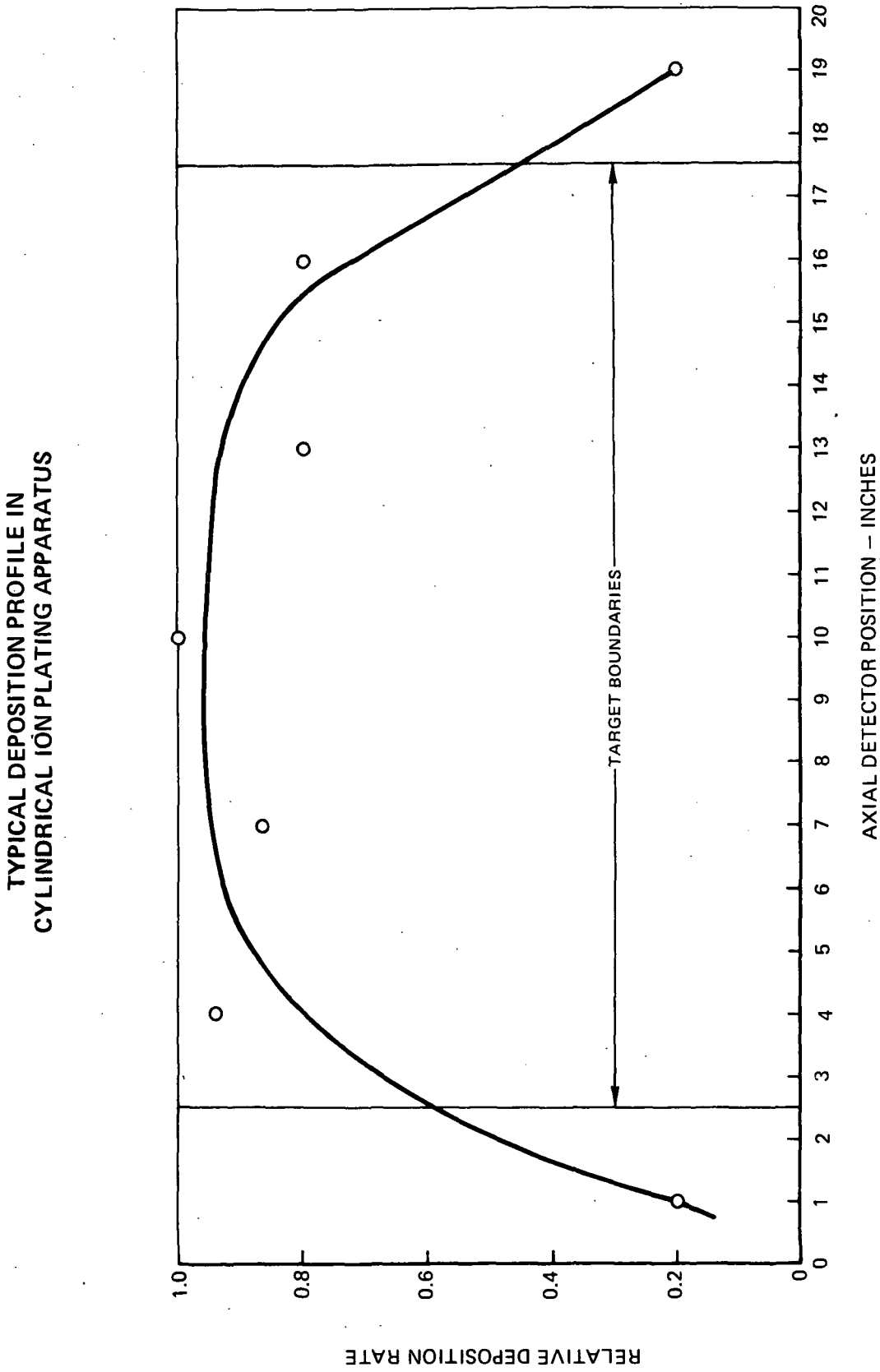
TYPICAL DEPOSITION PROFILE IN
CYLINDRICAL ION PLATING APPARATUS
RELATIVE DEPOSITION RATE
1.0
0.8
0.6
0.4
0.2
0
TARGET BOUNDARIES
0 1 2 3 4 5 6 7 8 9 10 11 12 13 14 15 16 17 18 19 20
AXIAL DETECTOR POSITION – INCHES

average value in this interval is much less than would be expected from other experiments on inwardly sputtering cylindrical cathodes. In their approximately 14 cm (5.5 inch long cylindrical cathode, Gill and Kay (Ref. 4) measured a variation of about ±20 percent from the average over the central 80 percent of the cathode.

Depositions were made with an axial magnet field strength of about 40 gauss. The magnetic field profile is shown in Fig. 3. This flat magnetic field profile was achieved using theory developed by Garrett (Ref. 5). The 40 gauss field was chosen because it produced a reasonable compromise between deposition rate and substrate heating. Lower magnetic fields, while lowering the substrate temperature, would also lower the deposition rate. Higher magnetic fields, while increasing the deposition rate to a point, would also raise the substrate temperature considerably.

Figure 4 shows the dependence of the fiber temperature as a function of target input power for several conditions. These temperatures were measured by placing a thin shielded thermocouple at various locations along the target axis at the radial position normally occupied by the fiber substrates. The assumption is made that the fiber reaches essentially the same temperature as the thermocouple did.

Test Procedures

Room temperature tensile tests were made using an Instron table model tensile testing machine as well as a fiber tensile tester designed and built at the United Aircraft Research Laboratories. The latter tensile tester was used to perform hot tensile tests by interposing a furnace between the fiber grips of the tester. This tensile tester is schematically illustrated in Fig. 5.

The 24-hour thermal exposures at temperatures up to 1200°C were performed using a fused silica tube inserted into a tube furnace and provided with a source of argon to maintain an inert atmosphere. The specimens to be heat treated were supported in high-purity alumina thermocouple tubes which were placed within the inert atmosphere in a small alumina crucible. The configuration of this arrangement is schematically shown in Fig. 6. During the thermal exposures, felted graphite was placed above the specimens but within the hot zone to act as an oxygen "getter" as a precaution against contamination from outgassing, back-diffusion, or contamination of the argon supply.

FIG. 3

AXIAL MAGNETIC FIELD STRENGTH IN
CYLINDRICAL ION PLATING APPARATUS

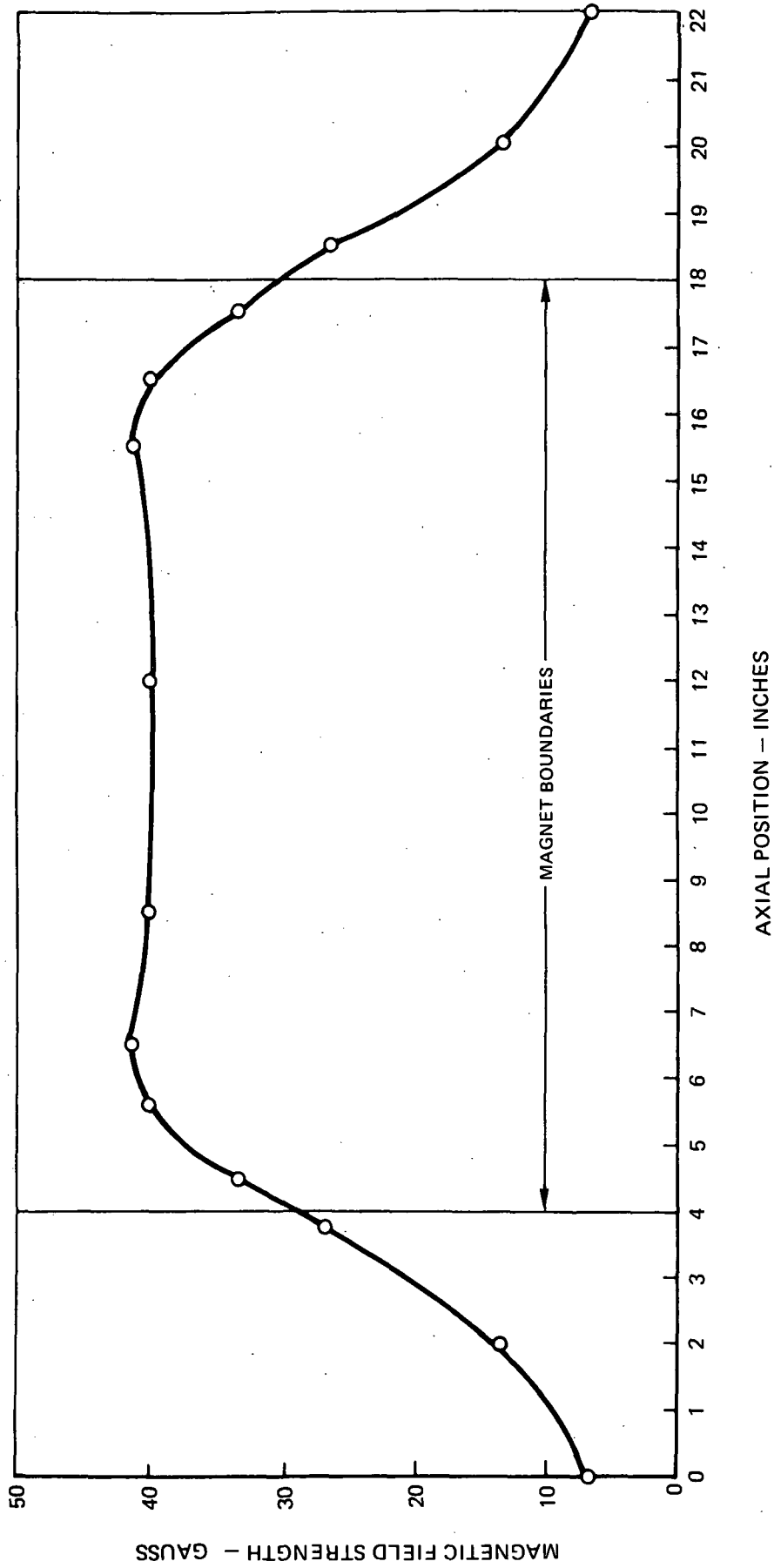

PROBE TEMPERATURE AT QUARTER INCH RADIUS OF CYLINDRICAL ION PLATING APPARATUS

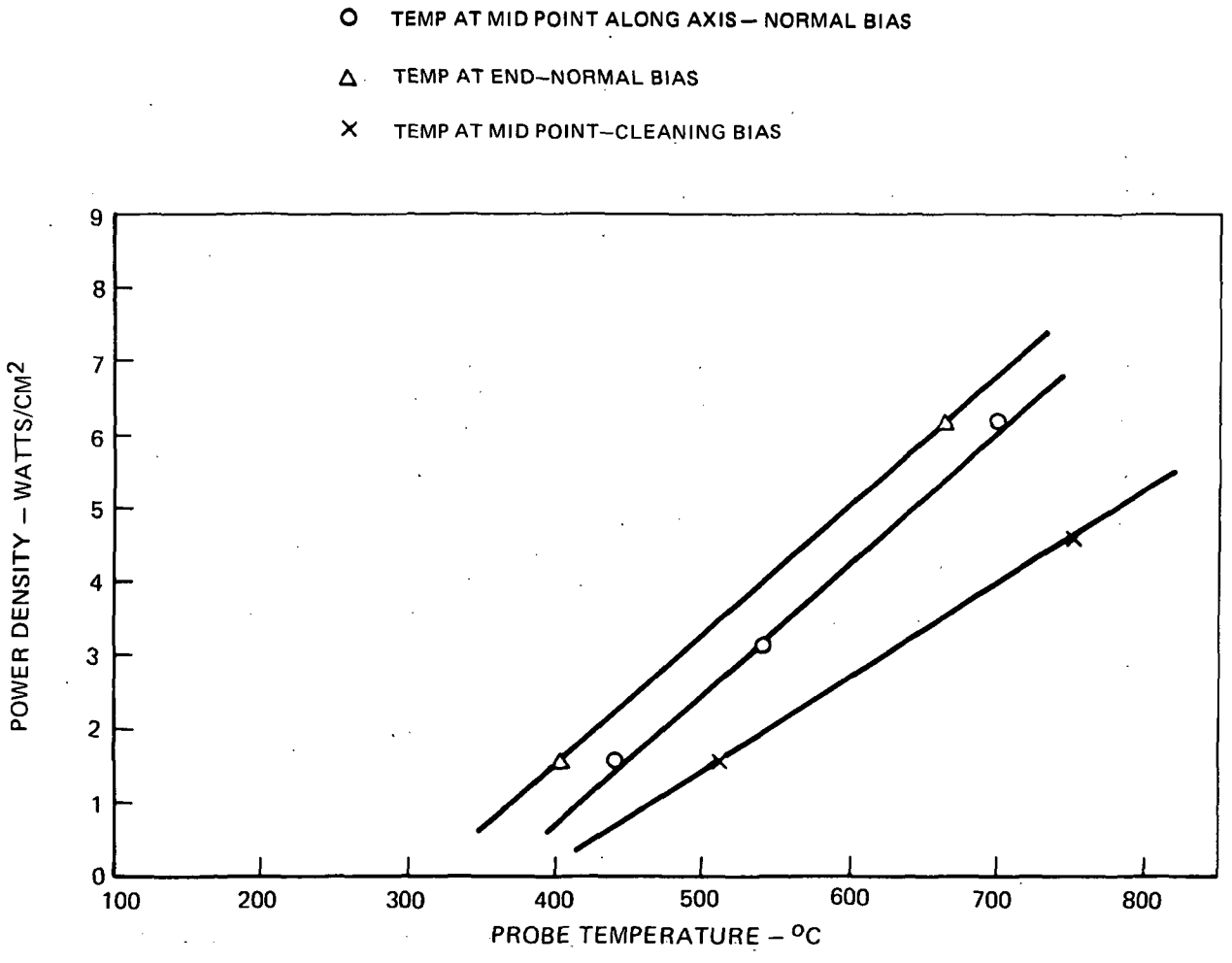

FIG. 6

SCHEMATIC DIAGRAM OF THE HOT TENSILE TESTER

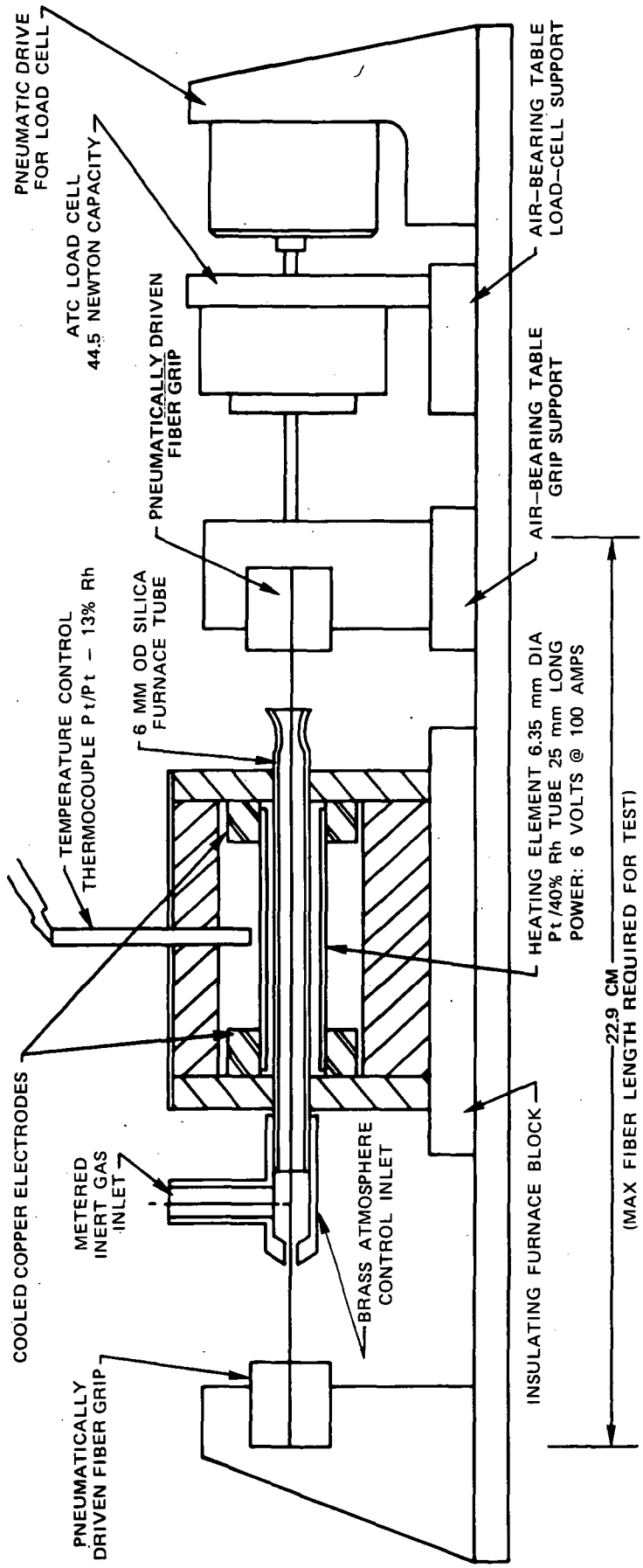

SCHEMATIC DIAGRAM OF THERMAL EXPOSURE UNIT

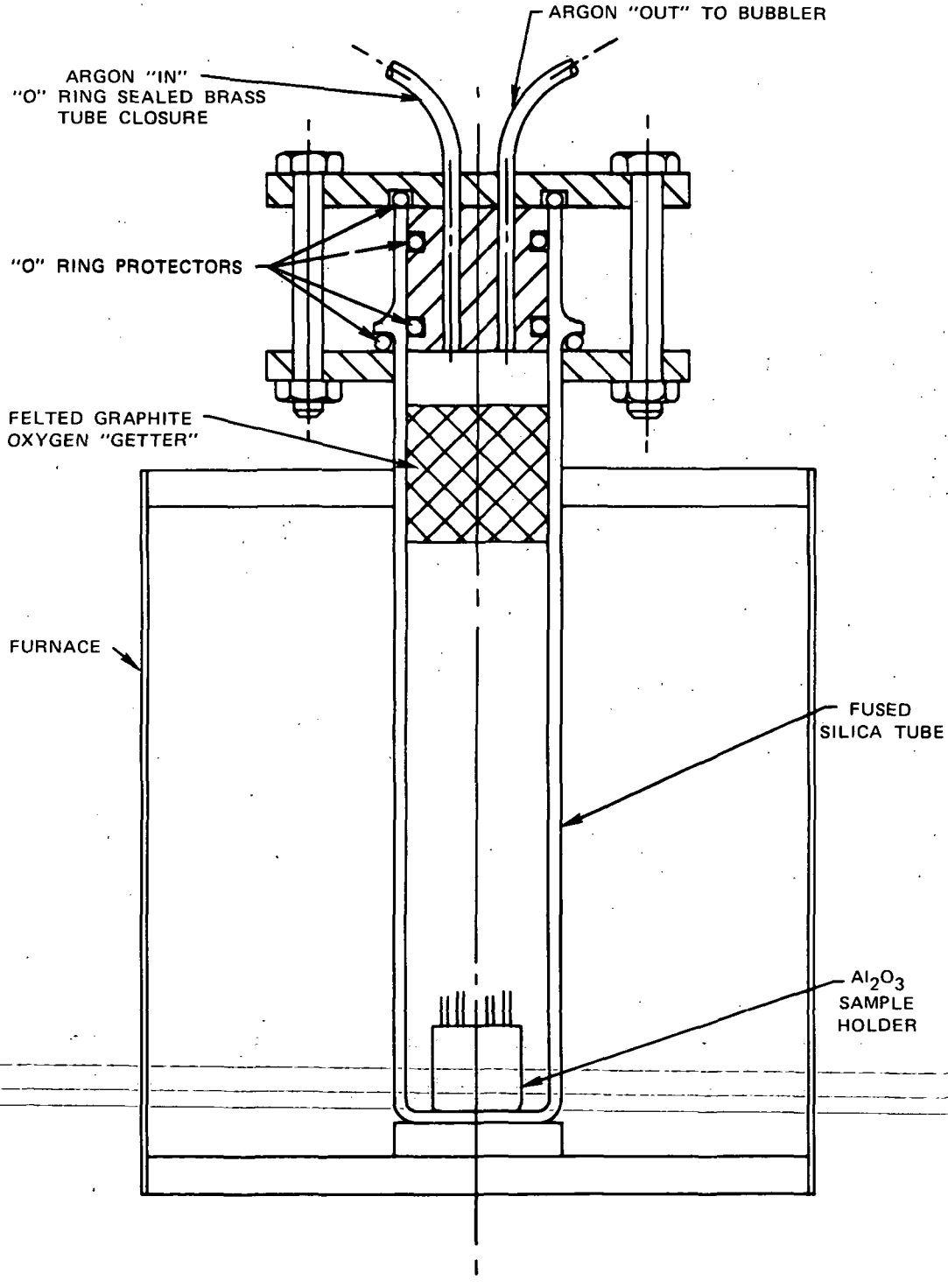

TEST RESULTS

The room temperature tensile tests were made on the fiber substrates as-received and after a variety of ion-plating operations and heat treatments. Tests performed on the fiber substrates, including those performed after 24-hour thermal exposures provide baseline data for evaluating the effects of the ion-plating process and thermal exposures of ion plated fibers by comparison. These baseline data are presented in Table III.

In Appendix I, all the individual data points are tabulated for which Table III is the summary. The scatter of the breaking forces led to an examination of the fracture surfaces of selected fibers using the SEM (scanning electron microscope), along with recording stress-strain curves. The fracture surfaces of tungsten fibers, both ion plated and as-received, showed flaw-initiated fractures to be associated with low values of tensile strength. This type of behavior is clearly seen in stress-strain curves, where flaw-initiated fractures occur at strength levels below those which produce plastic deformation. Two types of fracture surfaces are compared in Fig. 7 as recorded with the SEM; in one case, plastic deformation has reduced the diameter of the fiber prior to fracture, while in the other case, fracture was initiated at a flaw, giving the appearance of a brittle-fracture surface. The comparative stress-strain curves are presented in Fig. 8. These are illustrative of a large number of fracture surface examinations made using the SEM.

The niobium fiber always underwent plastic deformation prior to fracture. As shown in Fig. 9, the niobium fiber had "ears" approximately 180 degrees apart which were assumed to be the result of the wire-making process used. This feature probably did not affect strength measurements, but may have produced regions where the ion-plated barrier layers would be expected to be of poor quality.

The NASA-Hough carbon fiber appeared to have tensile strengths either above 152KN/cm^2 or below 124KN/cm^2; the average strength of 143KN/cm^2 thus has a large deviation. Fracture surfaces of this fiber are shown in Fig. 10.

A significant variation in the tensile strength measurements of the Tyco sapphire fiber also occurred. The range was from a high of 318KN/cm^2 to a low of 133KN/cm^2. This variation is apparently due to the sensitivity of the sapphire to surface flaws. A fracture surface of the sapphire fiber is shown in Fig. 11.

Effects of Thermal Exposure on the 25°C Tensile Properties of Fiber Substrates

As a part of the characterization of the effects of 24-hour thermal exposures on the tensile strength of the fiber substrates, pieces of the as-received fibers were subjected to the thermal exposures of 24-hour duration at 1100°C and at 1200°C. As expected, the tensile strength retained after the thermal exposures was lower than 100%. Table III summarizes the results which are itemized in Appendix I, and Table IV presents these as percentages of the tensile strength obtained prior to the thermal exposures.

Effects of Ion-Plated Barrier Layers on the 25°C Tensile Properties of Fiber Substrates

Further evaluation of the ion-plating process was achieved by subjecting the fiber substrates which were ion-plated with the candidate barrier materials to tensile tests at room temperature before and after 24-hour thermal exposure to temperatures of 1100°C and 1200°C. During the ion-plating process itself, the fiber substrates were subjected to temperatures of the order of 500°C for the duration of the plating process. The barrier layers were generally between 2 and 3 micrometers thick. The results of these tests are summarized in Table V.

Examination of the data in Table V shows that ion-plating the fibers tends to reduce their strength in the as-plated condition, although the degree of strength reduction is a function of the particular fiber and barrier layer. In the case of the tungsten fiber, the apparent loss of strength due to ion-plating varies from 5% to 50%. Since tungsten can be notch-sensitized by brittle coatings, the larger strength-loss values may be due to this effect. In addition, the ion-plated tungsten retains a higher percentage of its room temperature strength after exposure to elevated temperature than does the uncoated fiber. This suggests that the effect of thermal exposures on tungsten which result in a loss of strength at room temperature are surface effects against which the barrier layers are effective at high temperatures.

The niobium fiber appears to be less affected by the application of barrier layers by ion-plating than is the tungsten, since the greatest strength loss after plating is only 12%. The high temperature thermal exposures destroyed the Nb/TiC and Nb/WC-14Co specimens at both 1100°C and at 1200°C, and also destroyed the Nb/ZrC specimen at 1200°C. Those specimens which survived, however, compared well in retained strength to the heated but uncoated specimens. To compare the strength retention of niobium fiber after the 1100°C exposure, the breaking force value for the uncoated specimen was estimated from the data on the niobium at 1200°C and at room temperature, assuming its strength loss curve was similar to that of tungsten. This gave an estimated breaking force for uncoated niobium after a 24-hour exposure at 1100°C of 15.5 newtons. The measured value for the specimen exposed at 1100°C was 4.4 newtons, which appeared to be anomalously low.

TABLE III

Average 25°C Fiber Strength Before and After
24-Hour Thermal Exposures

Fiber	Diameter mm	Strength Values After Indicated Thermal Exposure					
		25°C		1100°C		1200°C	
		UTS	Force	UTS	Force	UTS	Force
Tungsten	0.127	287	37.4	158	29.4	114	22.8
Niobium	0.124	177	20.7	127*	15.5*	68	7.9
Sapphire	0.310	209	156	152	99.2	104	80.5
NASA-Hough Carbon	0.085	100	7.2	83	5.8	39	1.47

UTS in KN/cm^2; force in newtons; fiber diameter in millimeters

* estimated value

FRACTURE SURFACES OF TUNGSTEN FIBERS

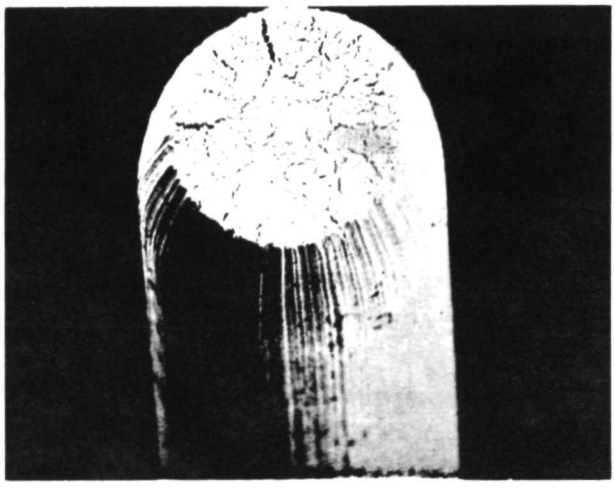

a) DUCTILE FRACTURE OF TUNGSTEN FIBER

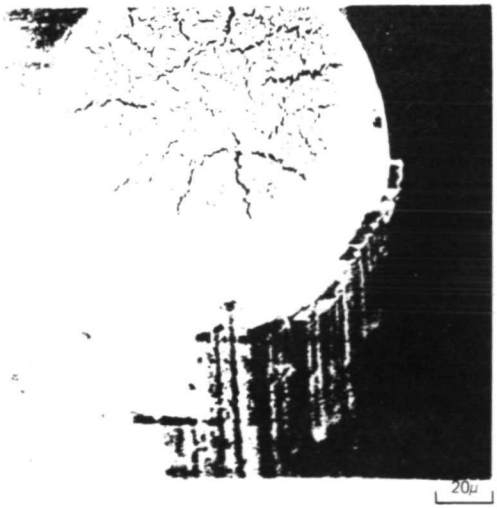

b) DUCTILE FRACTURE OF Al_2O_3 – COATED TUNGSTEN

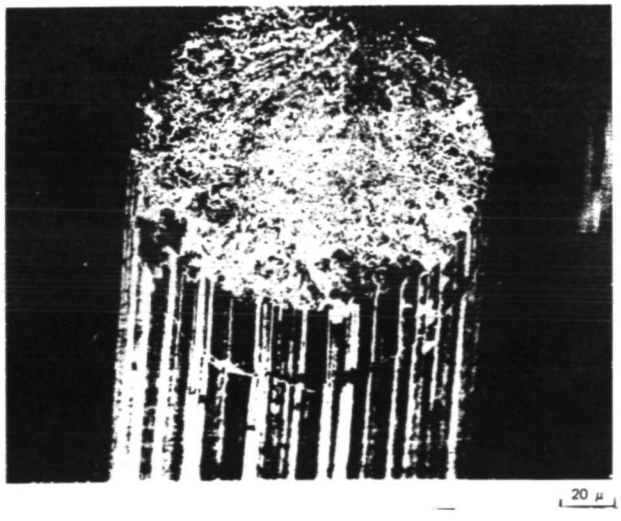

c) FLAW–INITIATED FRACTURE OF Al_2O_3 – COATED TUNGSTEN

STRESS–STRAIN CURVES FROM TENSILE FRACTURE SPECIMENS OF Al_2O_3–COATED TUNGSTEN

PULL RATE: 0.002 in./min.; GAUGE LENGTH=0.5 in.; ROOM TEMPERATURE TEST

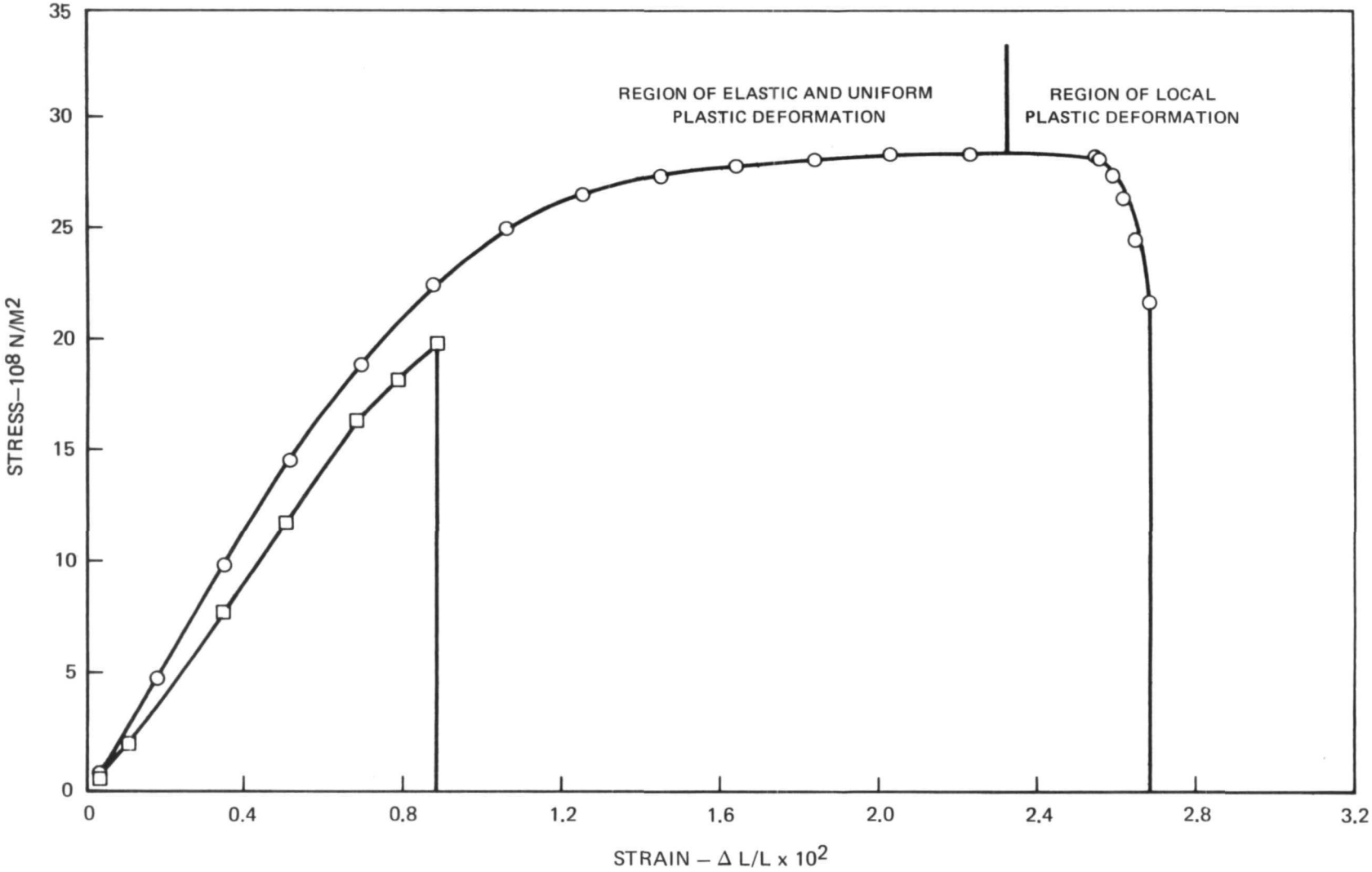

FIG. 8

FRACTURE SURFACE OF NIOBIUM FIBER

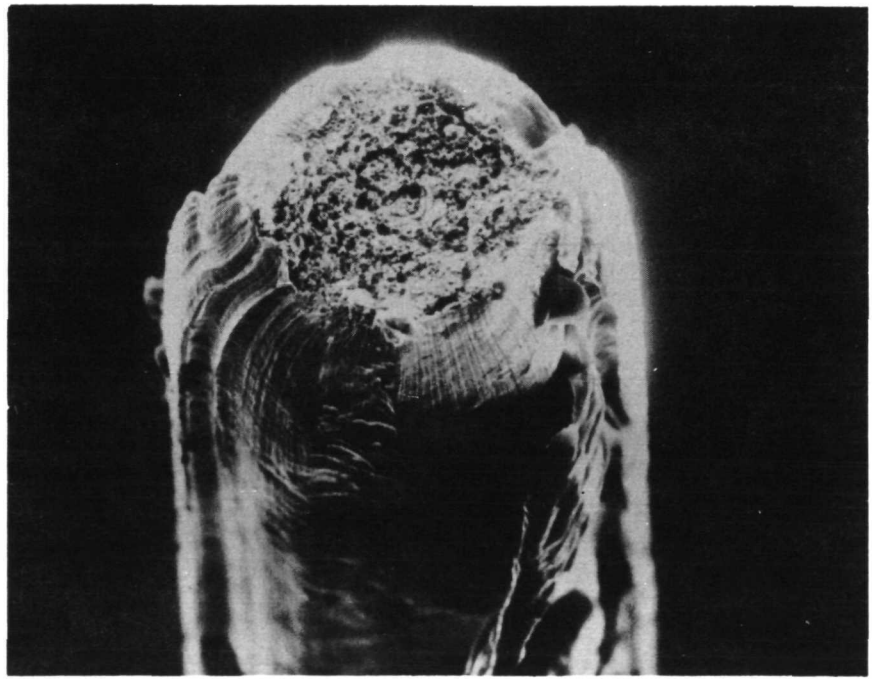

20μ

FRACTURE SURFACE OF NASA–HOUGH CARBON FIBER

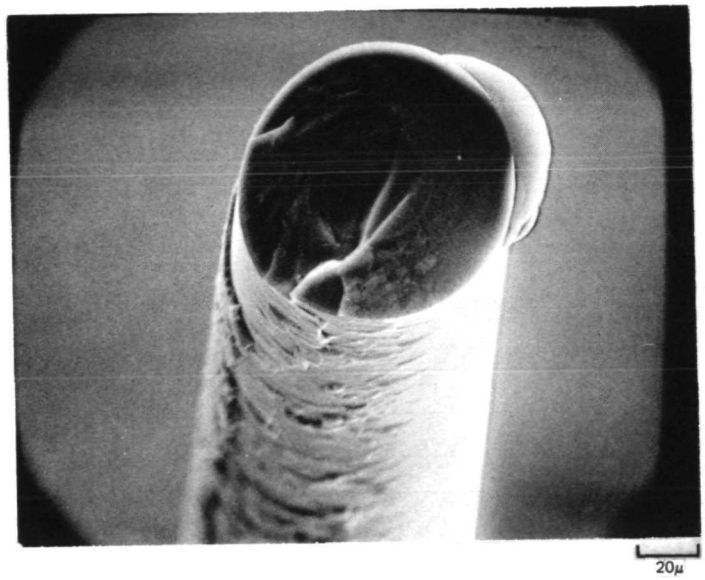

FRACTURE SURFACE OF TYCO SAPPHIRE FIBER

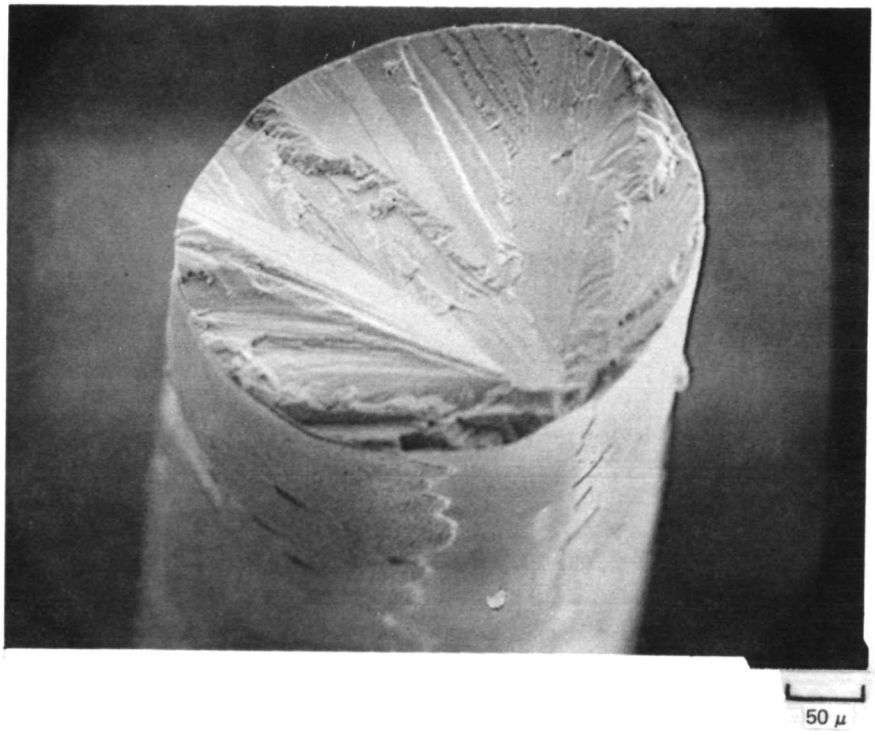

TABLE IV

25°C Value of Retained Strength After
24-Hour Thermal Exposures

Fiber	Strength After 1100°C Exposure	Strength After 1200°C Exposure
Tungsten	79%	61%
Niobium	72%*	38%
Sapphire	72%	50%
NASA-Hough Carbon	59%	27%

*estimated correct values (See Table III)

TABLE V

Average 25°C (Fiber/Barrier) Strength Before and After 24-Hour Thermal Exposures

Fiber/Barrier	25°C		1100°C			1200°C		
	Force Newtons	% of Uncoated	Force Newtons	% of 25°C Coated	% of 1100°C Uncoated	Force Newtons	% of 25°C Coated	% of 1200°C Uncoated
W/Al_2O_3	32.0	86	21.4	67	73	26.6	83	117
/Y_2O_3	30.7	82	29.7	97	100	29.7	97	130
/TiC	35.9	96	29.1	81	99	29.1	81	128
/ZrC	28.0	75	25.4	91	86	27.8	99	122
/WC-14Co	18.9	51	22.3	>100	76	22.3	>100*	98
Nb/Al_2O_3	19.6	95	12.5	64	80**	-	-	-
/Y_2O_3	18.5	89	7.4	40	48**	5.8	31	73
/TiC	19.7	95	-	-	-	-	-	-
/ZrC	18.2	88	15.1	83	97**	-	-	-
/WC-14Co	20.0	97	-	-	-	-	-	-
Sapphire/Y_2O_3	213	102	41.6	19.5	42	77.0	36.0	96
/TiC	258	123	94.3	37.0	95	94.3	37.0	117
/ZrC	203	97	145	71.4	146	77.0	38.0	96
/WC-14Co	23.7	11.3	184	(776)	185	145	(612)	180
N-HC/Al_2O_3	8.9	118	7.82	88	179	-	-	-
/Y_2O_3	3.1	41	7.65	247	175	-	-	-
/TiC	9.9	131	-	-	-	-	-	-
/ZrC	9.3	123	4.09	44	94	-	-	-
/WC-14Co	8.3	110	-	-	-	-	-	-

* > indicates "greater than"

** based on a breaking force of 15.5 newtons

The sapphire fiber yielded inconsistent and unpredictable breaking force data; however, it appears that the coatings may improve the sapphire by protecting it from surface flaws, as may also occur for tungsten. Examples of flaw-initiated fracture surfaces for sapphire and tungsten are presented in Fig. 12. Comparing the coated, heated fiber strength results to the uncoated, heated strength values for the sapphire, it is seen that the breaking forces for the coated fibers are generally higher than for the uncoated sapphire.

The NASA-Hough carbon fiber appears to sustain an improvement in strength from the ion-plating operations, as indicated by the strength comparisons in Table V. The strength retention after thermal exposure reflects this higher strength. However, the TiC and WC-14Co coated fibers broke up during the 1100°C thermal exposure, and all fibers tested broke up during the 1200°C thermal exposure.

Effects of Ion-Plated Metal Matrix Materials on the 25°C Tensile Properties of the Fiber Substrates

In order to determine the effectiveness of the candidate barrier layer materials to protect the fiber substrates from strength-reducing attack by nickel and titanium alloys, fiber substrates were ion-plated with IN600 nickel and Ti-6/4 titanium. The plated fibers were subjected to room temperature tensile tests before and after 24-hour thermal exposures at 1100°C and 1200°C (870°C for the Ti) for diffusion-protection evaluation. The results of the room temperature tensile tests on the metal plated fibers are summarized in Table VI.

The data collected in Table VI indicates that the ion-plated nickel, although a thick coating, does not contribute significantly to the strength of the resulting composite fiber at room temperature when tungsten and niobium are the fiber substrates. The over-coating of titanium does not appear to affect the strength of the tungsten fiber at room temperature, but does significantly increase the force required to break the niobium. Comparisons of the strength of heated, metal coated fibers to unheated, metal coated fibers and heated noncoated fibers were made ignoring the slight differences in the thickness of the nickel coatings on the specimens used. It is clear from Table VI that the nickel on the tungsten severely degrades the strength of the tungsten when the combination is heated, although there appears to be little difference between the 1100°C and 1200°C exposures for a 24 hour duration. The nickel coating on the niobium does not appear to have an effect after 24 hours at 1100°C, but results in catastrophic failure after 24 hours at 1200°C. The metal-coated sapphire fiber could not be tested at room temperature because of extreme brittleness; however, after thermal exposure at 1100°C and 1200°C, tensile tests could be made at room temperature which yielded approximately 50% of the strength recorded after similar thermal exposures of uncoated fiber. It is likely that the handling problem at room temperature was related to surface flaw sensitivity of the sapphire due to the metal plating, which was relieved by the thermal anneals. It is not clear, however, that the strengths found after the thermal anneals of the metal coated fibers were determined by surface flaws or by some reaction between the sapphire and the metal.

FLAW INITIATED TENSILE FRACTURES IN COATED TUNGSTEN AND SAPPHIRE FIBERS

a) W/WC–14Co/Ni

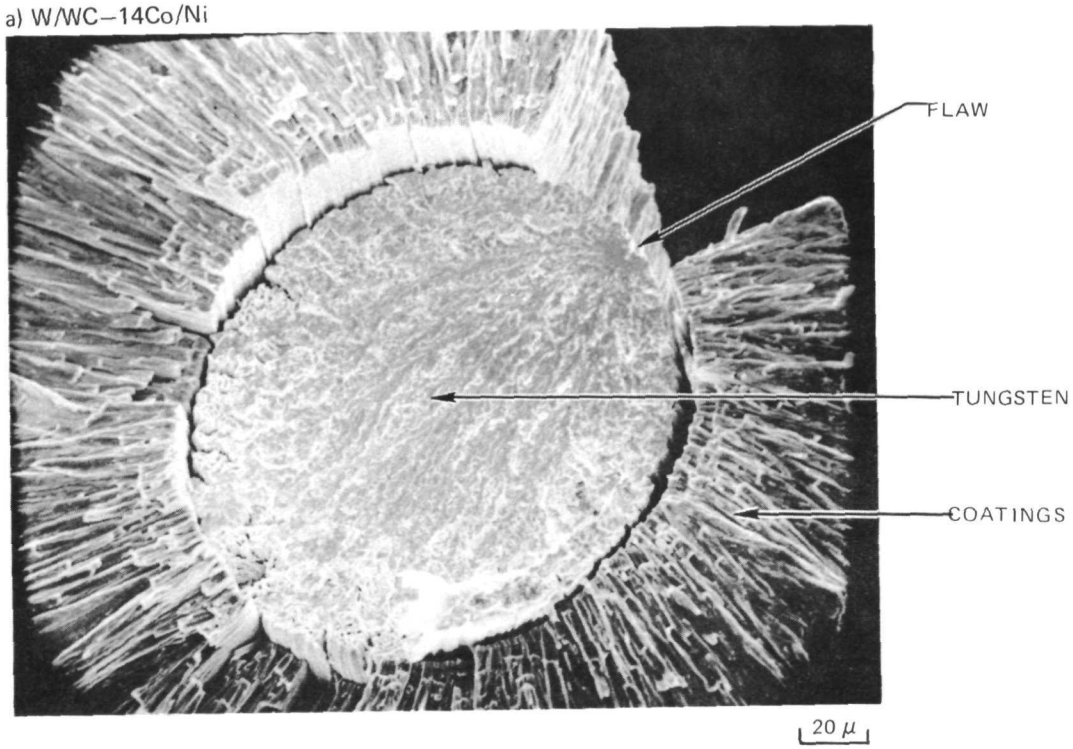

b) Al_2O_3/WC–14 Co/Ni

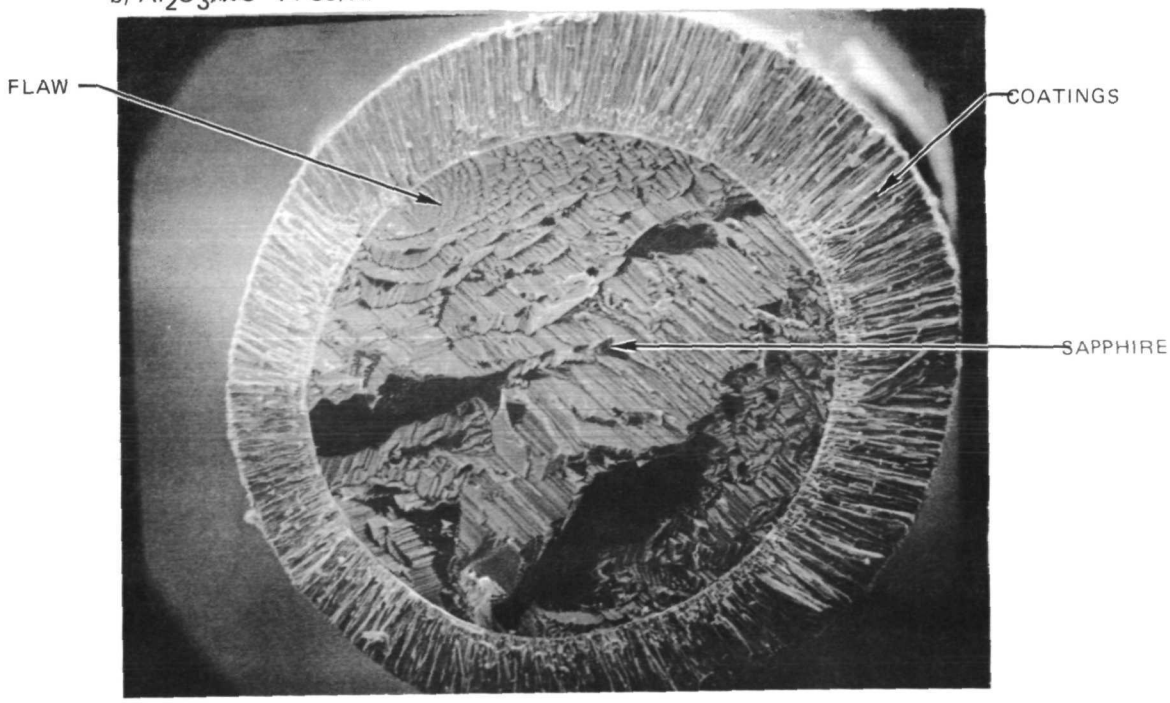

TABLE VI

Average 25°C Fiber/Metal) Strength Before and After 24-Hour Thermal Exposures

Fiber/Metal	Dia.(T)*	25°C Force Newtons	25°C % of 25°C uncoated	1100°C Force Newtons	1100°C % of 25°C coated	1100°C % of 1100°C uncoated	1200°C Force Newtons	1200°C % of 25°C coated	1200°C % of 1200°C uncoated
W/Ni	0.241	39.2	105						
	0.292(1100)			14.2	36	48			
	0.269(1200)						13.6	35	60
Nb/Ni	0.229	23.4	113						
	2.244(1100)			23.1	99	149	(fiber crumbled-) no test		
Al_2O_3/Ni	0.406	(fiber crumbled-) no test					49.8	--	62
	0.406(1100)			40.0		40			
N-HC/Ni	0.188	(no fiber) tested		8.67		199	(no test)		

Fiber/Metal	Dia. mm	25°C Force	25°C % of 25°C uncoated	870°C Force	870°C % of 25°C coated	% of 1100°C uncoated
W/Ti	0.192	37.36	100	33.94	91	115
Nb/Ti	0.203	37.81	183	15.96	42	103

*Parenthetical value indicates temperature of test for which the listed diameter was measured.

The strengths measured on the titanium-coated tungsten and niobium fibers before thermal annealing indicates that the titanium coating significantly raises the room temperature strength of the niobium/titanium composite above that of niobium alone, but has little effect on the tungsten. The thermal exposures at 870°C appear to affect the tungsten but little, while the niobium/titanium combination drops to 42% of its initial strength after the anneal.

Effects of Ion-Plated Barrier/Metal Coatings on the 25°C Tensile Strengths of Fiber Substrates Before and After Thermal Exposures

Tensile tests: Specimens of each substrate were ion-plated with each barrier layer material, and then overcoated with metal matrix material. Of the forty possible combinations, thirty-three were tested at room temperature prior to heat treatment. Two temperatures were chosen for thermal exposure of the nickel matrix coated fibers, and one temperature for the titanium coated fibers. Twenty-nine combinations were tested after each thermal exposure. Among these combinations, seventeen specimens were nickel-coated and exposed at 1100°C for twenty-four hours, fourteen were nickel-coated and exposed at 1200°C for twenty-four hours, and eleven were titanium-coated and exposed at 870°C for twenty-four hours. The strengths obtained at 25°C for these test specimens are summarized in Table VII.

The variations in the breaking force of fiber substrate subjected to ion-plating of both barrier layers and matrix materials after the thermal exposures indicate that a variety of factors are involved in determining the final strength of the plated fiber. It appears that various interactions occur among the materials, some of which may be annealing of strains set up during the ion plating process. For example, as-received tungsten retains some 86% of its virgin fiber strength after being ion-plated with aluminum oxide. After thermal exposure for 24 hours at 1200°C, the uncoated tungsten reatains only 61% of its original 25°C tensile strength, whereas the Al_2O_3 coated fiber retains 83% of its 25°C strength; this latter value is 117% of the strength retained by the virgin tungsten after the heat treatment. When tungsten is coated with nickel and heat treated, the 25°C strength is significantly lower than after similar heat treatment of tungsten only (36% of the after-1200°C retained strength of tungsten). When coated with both aluminum oxide and nickel, and exposed to 1200°C for twenty four hours, the combination retains 51% of its original room temperature strength, and compared to uncoated tungsten thermally treated, has dropped to 85% of the after-1200°C tungsten strength. In order of retained strength after 1200°C thermal exposure, then, the ranking of the various tungsten-coating combinations is

tungsten/aluminum oxide
tungsten
tungsten/aluminum oxide/nickel
tungsten/nickel

TABLE VII

Average 25°C (Fiber/Barrier/Matrix) Strength After 24-Hour Thermal Exposure

Material	Dia. mm	25°C Force Newtons	25°C % 25°C Uncoated	1100°C Force Newtons	1100°C % 25°C Coated	1100°C % 1100°C Uncoated	1200°C Force Newtons	1200°C % 25°C Coated	1200°C % 1200°C Uncoated
W/Al_2O_3/Ni	.241	37.5	100				19.3	51	85
W/Y_2O_3/Ni	.287	37.3	100	25.8	69	88	18.7	50	82
W/TiC/Ni	.244	37.5	100	12.0	32	41	24.0	64	105
W/WC-14Co/Ni	.254	36.0	100	--	--	--	27.1	75	119
W/ZrC/Ni	.248	37.5	100	11.1	30	38	8.5	23	37
Nb/Al_2O_3/Ni	.188	20.1	97	25.7	>100	166	18.9	94	239
Nb/Y_2O_3/Ni	.249	20.4	99	--	--	--	20.9	>100	265
Nb/TiC/Ni	.249	20.2	98	16.3	81	105	18.9	93	237
Nb/WC-14Co/Ni	.259	19.8	96	30.2	>100	179	16.3	82	206
Nb/ZrC/Ni	.272	19.9	96	30.2	>100	195	19.3	97	244
N-HC/Al_2O_3/Ni	.237	N O	T E S T	15.6	--	269	--	--	--*
N-HC/TiC/Ni	.196	6.7	93	--	--	--	--	--	--
N-HC/WC-14Co/Ni	.235	10.2	142	2.3	23	40	--	--	--
N-HC/ZrC/Ni	.196	9.3	129	7.7	83	133	--	--	--
Tyco/Y_2O_3/Ni	.417	19.6	12.6	49.8	>100	50	54.3	>100	55
Tyco/TiC/Ni	.417	134.3	86	24.2	18	24	97.9	73	99
Tyco/WC-14Co/Ni	.457	19.9	12.8	43.1	>100	43	894	>100	900
Tyco/ZrC/Ni	.472	4.1	2.6	74.7	>100	75	50.0	>100	50

* Blank spaces indicate no fiber survived the thermal exposure.

TABLE VII (Cont'd.)

Material	Dia. mm	25 C Force Newtons	25 C % 25 C Uncoated		870 C Force Newtons	870 C % 25 C Coated
W/Al_2O_3/Ti	.192	37.4	100		33.9	91
W/TiC/Ti	.193	51.6	>100		39.7	77
W/WC-14Co/Ni	.251	74.1	>100		33.8	46
W/ZrC/Ti	.262	80.1	>100		33.6	42
Nb/Al_2O_3/Ti	.203	37.8	>100		15.8	42
Nb/TiC/Ti	.203	31.1	>100		20.5	66
Nb/WC-14Co/Ni	.193	34.7	>100		22.3	64
N-HC/TiC/Ti	.169	12.2	>100		--	--
N-HC/ZrC/Ti	.151	10.7	>100		--	--
Tyco/Y_2O_3/Ti	.363	107.6	69		83.2	77
Tyco/TiC/Ti	.371	144.6	93		73.4	51
Tyco/WC-14Co/Ni	.345	195.7	>100		67.6	35
Tyco/ZrC/Ti	.413	75.6	48		86.7	115

When comparisons are made as above on all the tested fiber-material combinations, the ranking of the materials according to strength is as listed in Table VIII. On the basis of this tabulation, the barrier layers which result in fiber/barrier/metal strengths at 25°C after thermal exposure for 24 hours at 1200°C which are greater than or equal to the strengths retained by the uncoated fibers subjected to the same thermal exposure are listed in the order of decreasing strength after 1200°C thermal exposure.

Hot Tensile Tests

Hot tensile tests were performed on fiber specimens of adequate length which remained after other tests had been performed. The test consisted of a nine minute exposure to a temperature of 860 ± 10°C for nine minutes plus loading to fracture at temperature after the nine minute exposure. The specimens tested are listed in Table IX, with comparative loads obtained on similar specimens of fiber before and after thermal thermal exposures lasting 24 hours.

From the data in Table IX, it is seen that tungsten, tungsten/yttria, and tungsten/tungsten carbide-cobalt exhibit the same hot tensile strength, which is about half that at room temperature, and somewhat lower than the strength retained at room temperature after 24 hours at 1200°C. The yttria coated tungsten and the tungsten carbide-cobalt coated tungsten overcoated with titanium have hot tensile strengths approximating the room temperature strengths, and somewhat higher than the room temperature strengths retained after 24 hours at 870°C.

The niobium with various overcoats appears to obtain reasonable protection from any weakening effects of the metal overcoats, while the barrier layers alone yield tensile strengths for the coated niobium approximately equal to the strengths for uncoated niobium.

Long-Term Diffusion Tests

In order to enhance the diffusion of the materials in the fiber/barrier/metal combinations, selected fibers were thermally exposed to temperatures betwen 1200°C and 1300°C for 136 hours. The strengths measured on these fibers at room temperature after the thermal exposure are listed in Table X.

The data in Table X represent the results of a very severe diffusion protection test. It can be seen that respectable strengths remain for both the tungsten and niobium fibers after this long-time, high temperature exposure.

Non-Destructive Evaluation

The specimens which were subjected to the long-time, high temperature exposures were mounted at an angle of 80° from the vertical, sectioned, and examined with the electron microprobe to obtain distributions of the elements which may have diffused during the exposure.

TABLE VIII

Listing of Fiber/Barrier/Matrix Systems in Order of Retained Strength Relative to Unprotected Substrate After 24-Hour Thermal Exposure

Material	Barrier	% Strength Retained	Temp. of Exposure
W/Barrier/Ni	WC-14Co	119	1200°C
	TiC	105	
	Al_2O_3	85	
	Y_2O_3	82	
	ZrC	37	
Sapphire/Barrier/Ni	WC-14Co	900	
	TiC	99	
	Y_2O_3	55	
	ZrC	50	
Nb/Barrier/Ni	Y_2O_3	265	
	ZrC	244	
	Al_2O_3	239	
	TiC	237	
	WC-14Co	206	
NASA-Hough Carbon/Barrier/Ni	Al_2O_3	269	1100°C
	ZrC	133	
	WC-14Co	40	
W/Barrier/Ti	Al_2O_3	91	870°C
	TiC	77	
	WC-14Co	46	
	ZrC	42	
Sapphire/Barrier/Ti	ZrC	115	
	Y_2O_3	77	
	TiC	51	
	WC-14Co	35	
Nb/Barrier/Ti	TiC	66	
	WC-14Co	64	
	Al_2O_3	42	
NASA-Hough Carbon/Barrier/Ti	- None		

TABLE IX

860°C Tensile Strengths with Comparative Data

Fiber	860°± 10°C Break Force Newtons	25°C Break Force - as-plated Newtons	25°C Break Force After Thermal Exposure Newtons	deg. C
W/Y_2O_3	17.8	30.7	29.7	1200
W/WC 14Co	17.8	18.9	22.3	1200
Nb/Y_2O_3	5.47	18.5	5.8	1200
Nb/Al_2O_3	18.1	19.6	12.5	1100
Nb/WC-14Co	11.8	20.0	----------	
$Nb/Y_2O_3/Ni$	16.9	20.4	20.9	1200
Nb/ZrC/Ni	13.3	19.9	19.3	1200
Nb/TiC/Ni	16.4	20.2	18.7	1200
$W/Al_2O_3/Ti$	34.4	37.4	33.9	870
W/WC-14Co/Ti	34.4	74.0	22.3	870
Nb/TiC/Ti	19.3	31.1	20.5	870
Nb/WC-14Co/Ti	18.7	34.7	22.3	870
$Nb/Al_2O_3/Ti$	18.7	37.8	15.8	870
W	17.8	37.4	22.8	1200
Nb	3.9	20.7	7.9	1200

TABLE X

Average 25°C Strengths of Selected Fibers Before and After 136- Hour Thermal Exposure at 1200 - 1300°C

Fiber	25°C unheated Force Newtons	1200°C 24 hours Force Newtons	1200 - 1300°C 136 hours Force Newtons
W/Al_2O_3/Ni	37.5	19.3	18.9
W/Y_2O_3/Ni	37.3	18.7	5.43
W/TiC/Ni	37.5	24.0	18.0
W/ZrC/Ni	37.5	8.5	16.7
Nb/ZrC/Ni	19.9	19.3	8.45
Nb/Al_2O_3/Ni	20.1	18.9	5.34
N-HC/Al_2O_3/Ni			did not survive
N-HC/ZrC/Ni			did not survive

DISCUSSION

The fractography studies made using the SEM to examine the fracture surface of tensile tested specimens indicate clearly that the ion-plated coatings were very adherent to the tungsten and niobium fibers, while the adherence to the sapphire was apparently adequate, but the adherence to the NASA-Hough carbon was marginal. In addition, many of the tungsten fractures were surface-flaw initiated after the ion-plating process was used. This is consistent with the known tendency of tunsten to be notch-sensitized by the application of brittle coatings. The fractures observed with the sapphire fibers were also largely flaw-initiated. A wide scatter of breaking forces was recorded, but it is noteworthy that the titanium carbide coating on the sapphire appears to significantly improve its strength. This may be due to a reduction in the sensitivity of the sapphire to its surface condition.

Element distribution scans were made on nickel-coated tungsten fibers thermally exposed for 24 hours at 1100°C and 1200°C for comparison with the longer thermal exposures. For the microprobe examination, the fibers were cut at 80° from a transverse section, resulting in a magnification (maximum) of 5.76. The line scans to determine the distribution of matrix metal material were made through the region of greatest magnification, which must be taken into account when interpreting the degree of apparent diffusion and the distribution of the elements. The expected penetration of nickel into the tungsten fiber, after 24 hours, is shown in Figs. 13 and 14. When a 2 micrometer thick barrier layer was supplied by ion-plating the tungsten fiber, the penetration of nickel was significantly reduced, and in some cases, prevented. These results are itemized below.

The combination W/TiC/Ni heated for 24 hours at 1200°C was examined with the electron microprobe, with the results presented in Figs. 15 and 16. Some diffusion of nickel can be observed.

The combination W/Y_2O_3/Ni heated for 24 hours at 1200°C showed no diffusion of the nickel, as shown in Figs. 17 and 18.

The combination W/Al_2O_3/Ni heated for 24 hours at 1200°C showed no penetration of the nickel into the tungsten fiber, as illustrated by Fig. 19; a 136 hour exposure at temperatures between 1200°C and 1300°C shows little penetration of the nickel into the tungsten fiber, although it is found in the aluminum oxide barrier-layer region, see Fig. 20. The recrystallization of the tungsten can be observed in this figure. The line scans of these specimens are shown in Fig. 21. The breaking force for this combination after 136 hours at 1200°-1300°C was 18.9N, which compared well with 19.3N after only 24 hours at 1200°C.

These results suggest that both Y_2O_3 and Al_2O_3 are adequate barrier materials in thicknesses of approximately 2 micrometers against the diffusion of nickel into tungsten. The 136 hour thermal exposure was a particularly severe test of the ability of the ion-plated aluminum oxide barrier to act as a diffusion barrier. An analysis by electron microscope diffraction of the crystal structure of the aluminum oxide barrier layer after the 136 hour high temperature exposure yielded a pattern of alpha-aluminum oxide (the stable, room temperature form) with no other phases present. The structure of the as-ion-plated aluminum oxide film on tungsten was previously analyzed and identified as the gamma or eta phase (a high temperature form). Although the electron microprobe analysis shows the presence of nickel in the aluminum oxide barrier layer region, the nickel does not appear to have affected the structure of the aluminum oxide.

The diffusion studies made using the electron microprobe indicate that little diffusion of the metal matrix material penetrates the barrier layers, in general, and in particular show that aluminum oxide and yttrium oxide are very resistant to penetration by nickel. Examination of the 136-hour exposure of aluminum oxide-protected tungsten fiber shows that almost no nickel penetrated the 2 micrometer thick barrier layer.

DISTRIBUTION OF Ni AND W IN NICKEL–COATED TUNGSTEN FIBERS

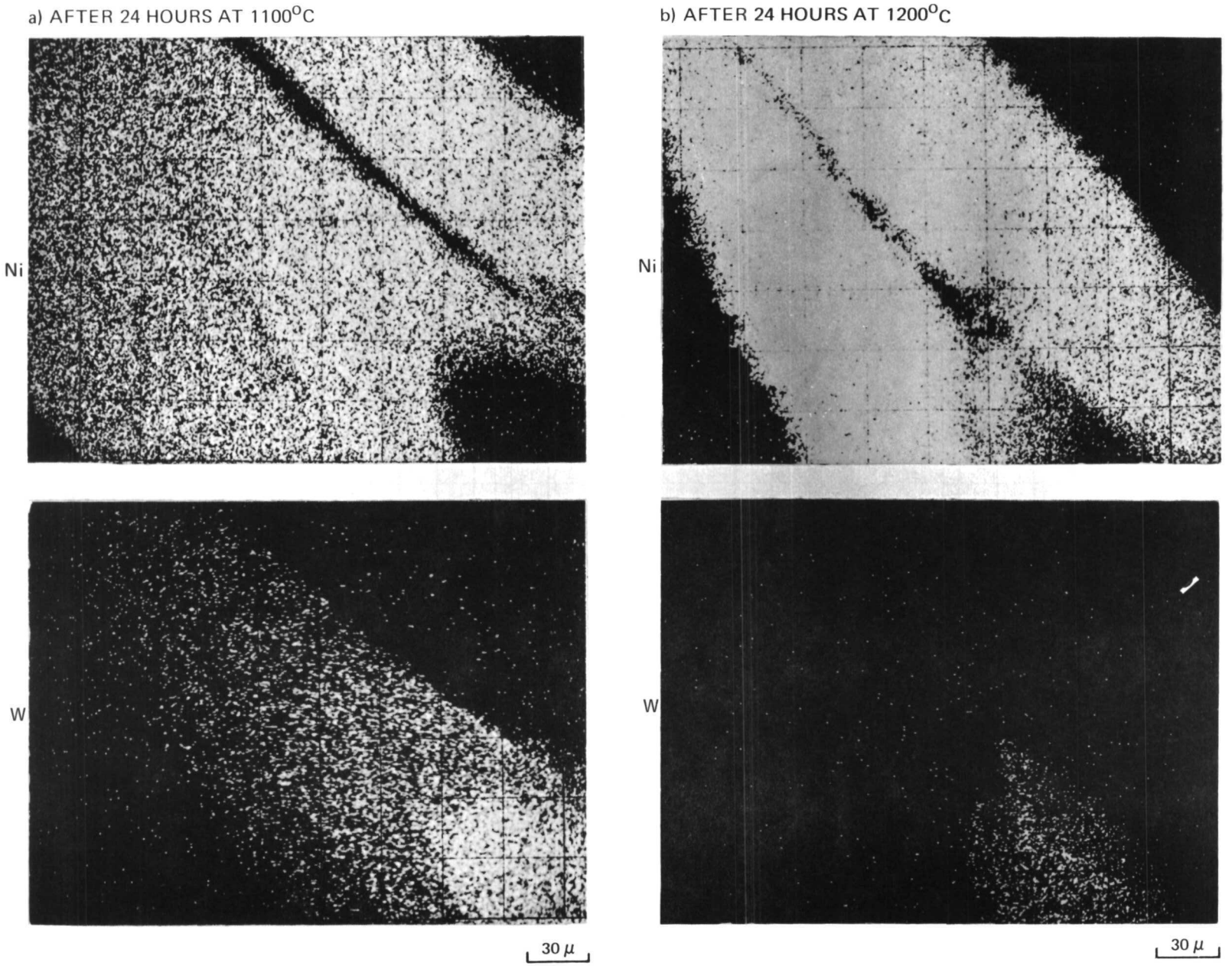

FIG. 13

ELEMENT LINE SCANS FOR W AND Ni IN NICKEL–COATED TUNGSTEN

LINEAR MAGNIFICATION 5.76

a) AFTER 24 HOURS AT 1100°C

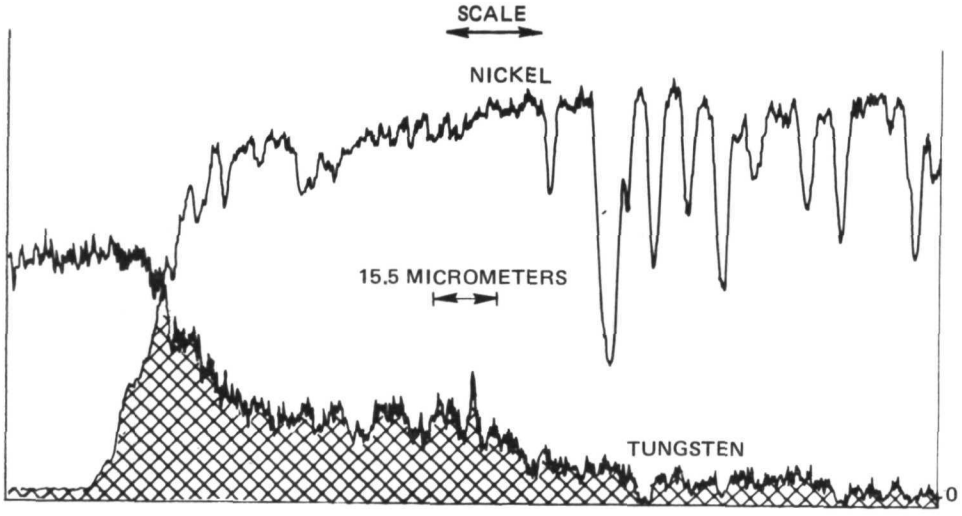

b) AFTER 24 HOURS AT 1200°C

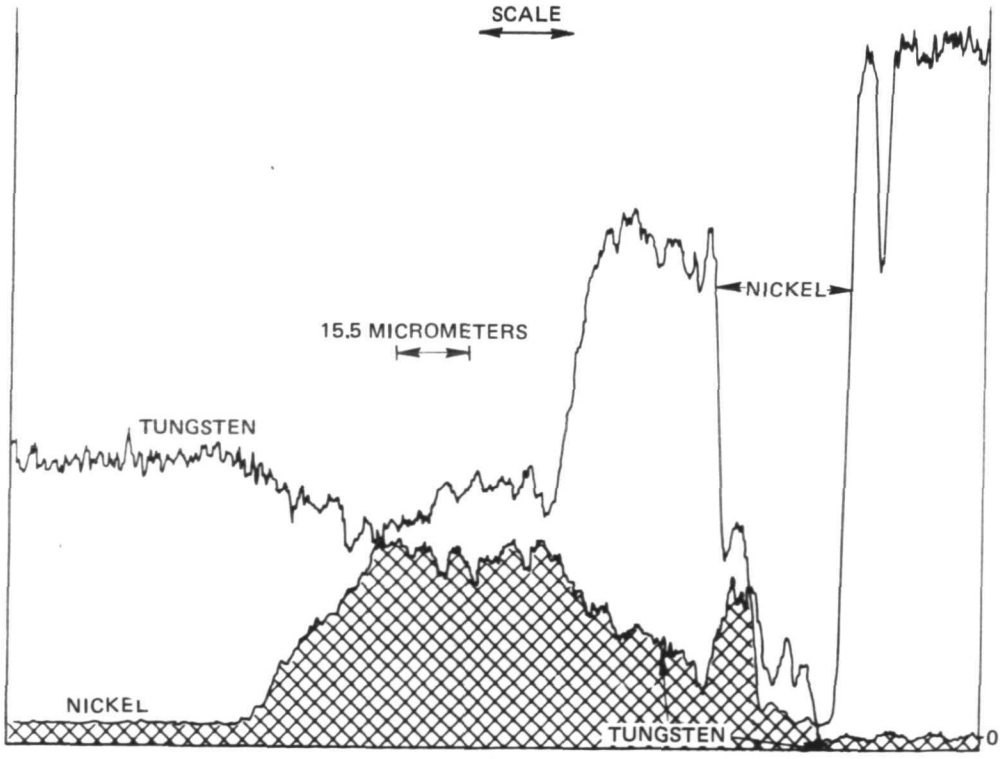

ELEMENT DISTRIBUTIONS IN W/TiC/Ni AFTER 24 HOURS AT 1200° C

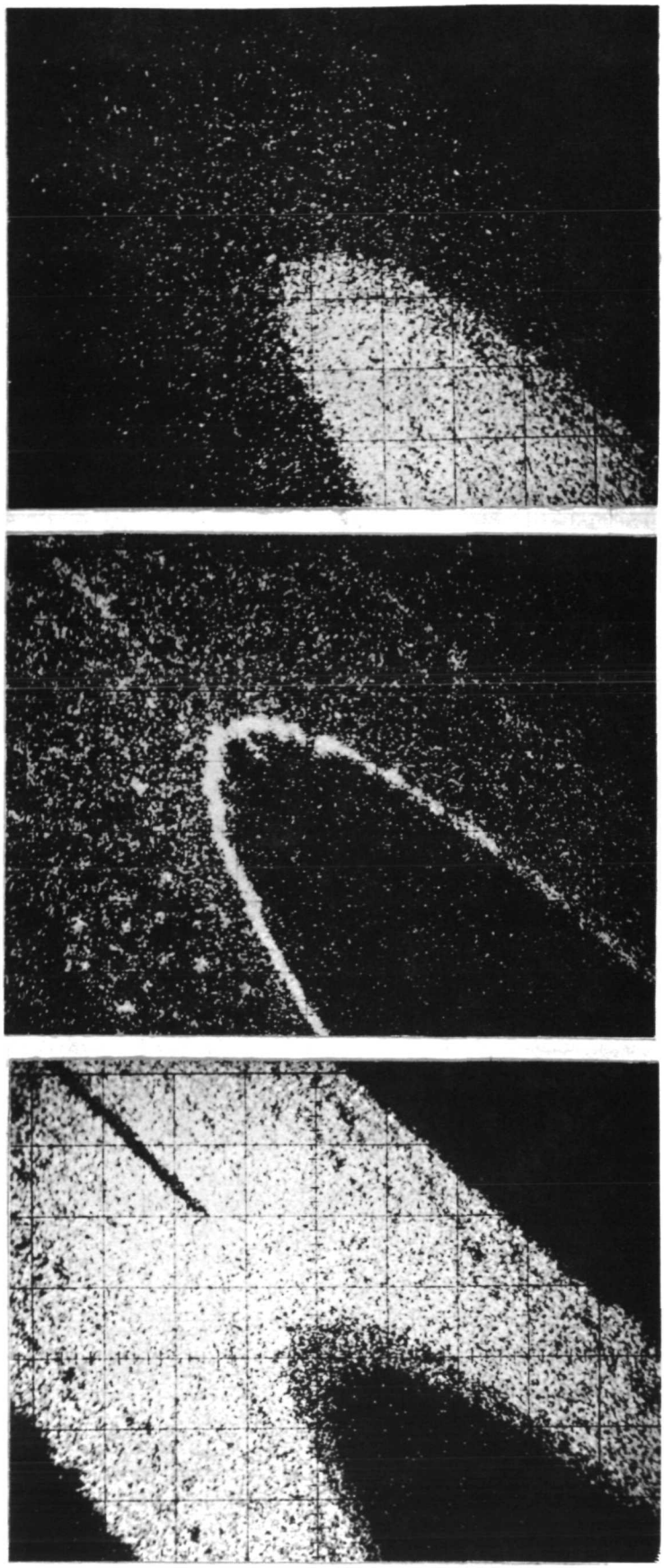

ELEMENT LINE SCANS FOR W AND Ni IN W/TiC /Ni AFTER 24 HOURS AT 1200° C

LINEAR MAGNIFICATION 5.76

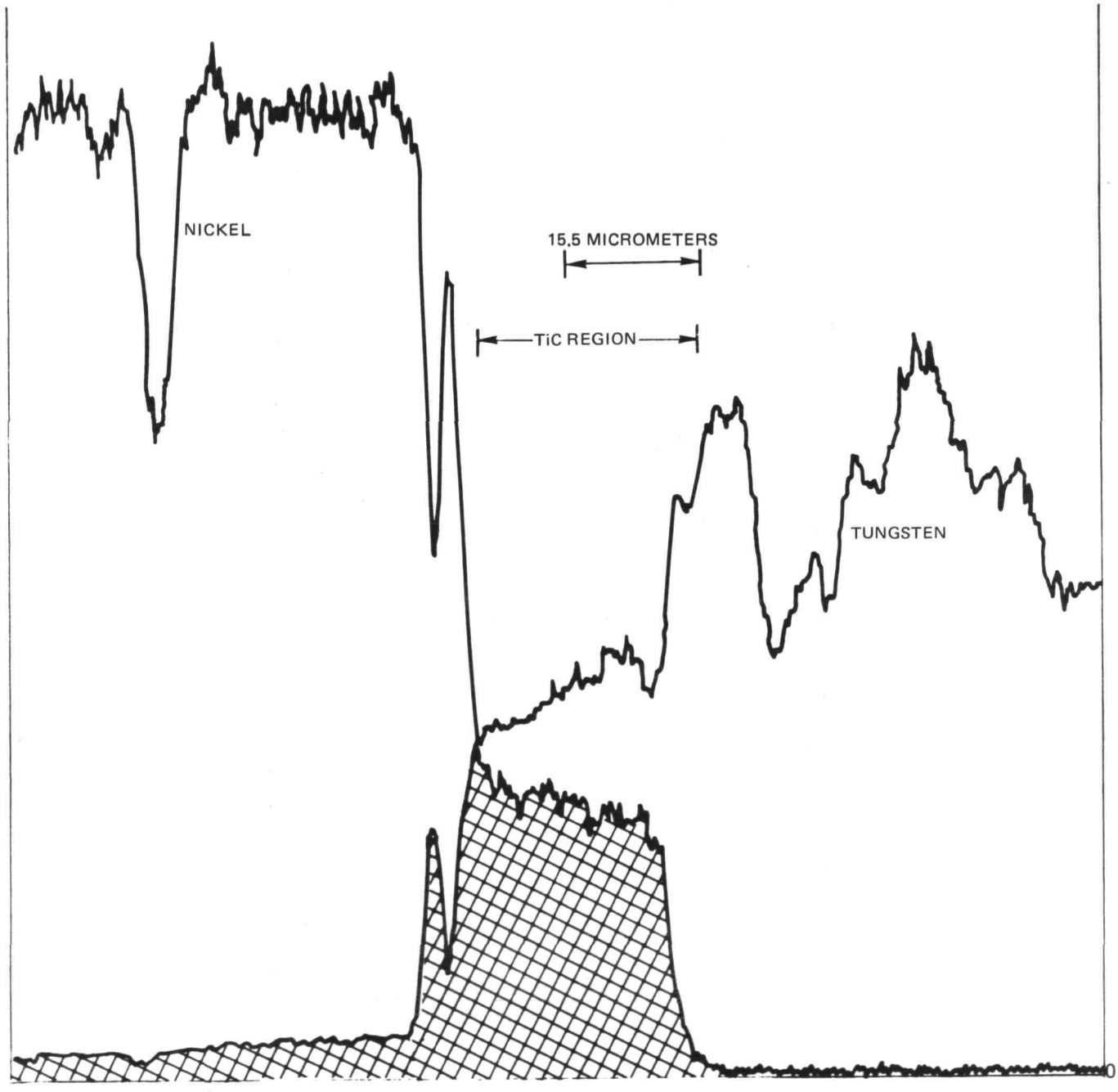

ELEMENT DISTRIBUTIONS IN $W/Y_2O_3/Ni$
AFTER 24 HOURS AT 1200° C

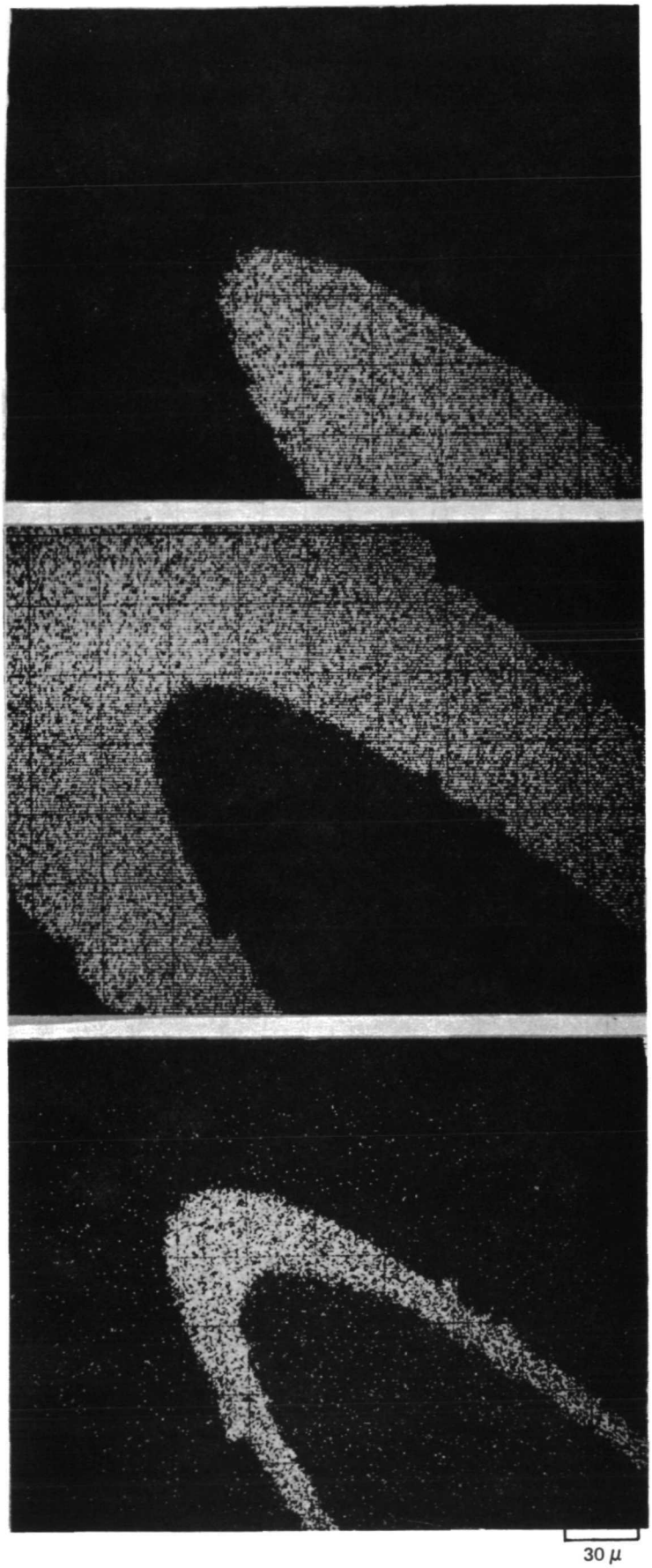

ELEMENT LINE SCANS FOR W AND Ni IN $W/Y_2O_3/Ni$ AFTER 24 HOURS AT 1200°C

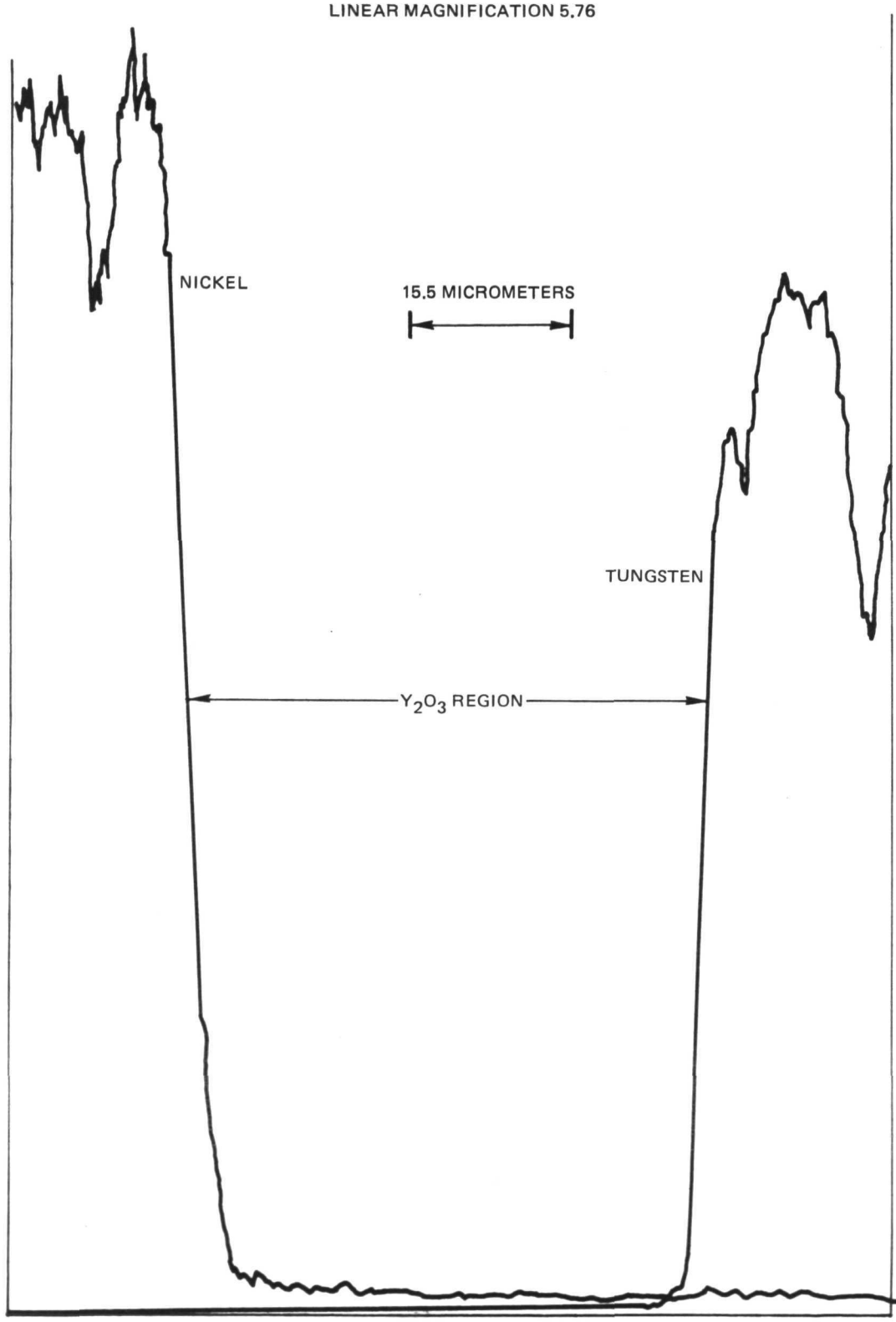

FIG. 19

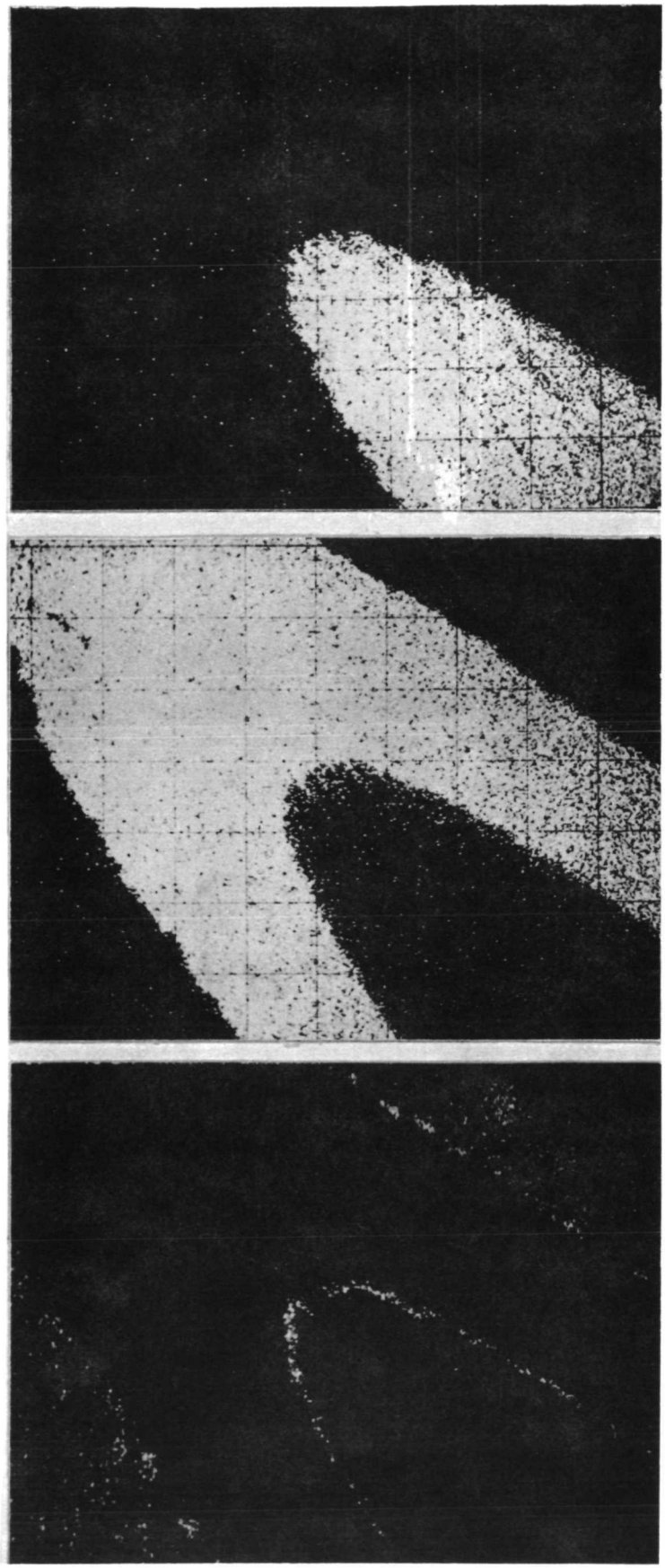

DISTRIBUTION OF ELEMENTS IN $W/Al_2O_3/Ni$ AFTER 136 HOURS AT 1200 –1300 C

ELEMENT LINE SCANS FOR W AND Ni IN W/Al_2O_3/Ni

LINEAR MAGNIFICATION 5.76

a) AFTER 24 HOURS AT 1200°C

b) AFTER 136 HOURS AT 1200–1300°C

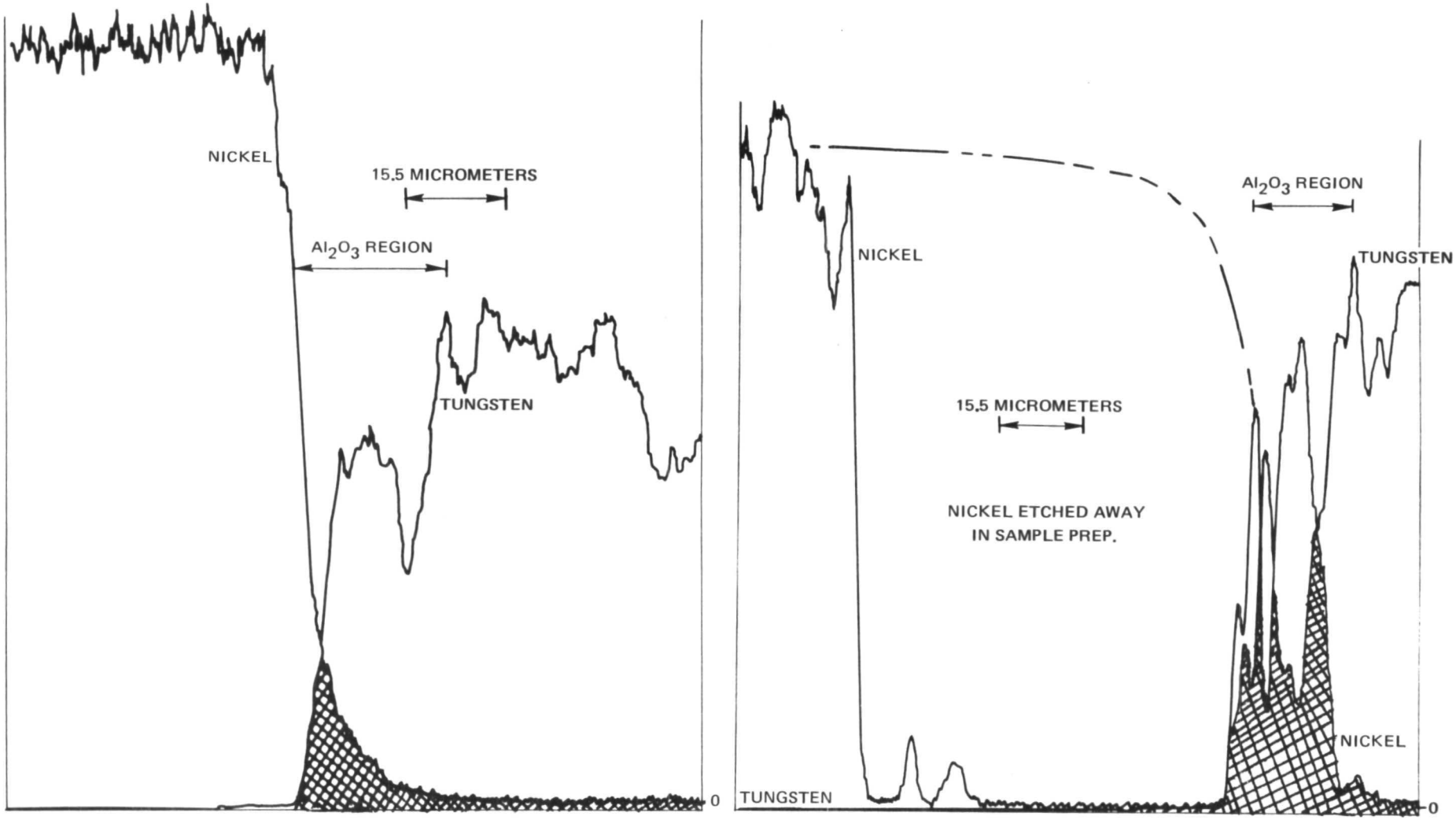

FIG. 21

CONCLUSION

The survey of barrier layer materials and fiber substrates conducted under this program indicates that successful combinations of fibers and barrier materials can be produced which will maintain sufficient strength to reinforce nickel and titanium alloys after the fabrication of fiber-reinforced metal matrix composites.

The above conclusion is based on the results of room temperature tensile tests performed on the fibers coated with the barrier materials, the metal matrix materials and the barrier coated fibers coated with the metal matrix materials after a variety of thermal exposures, as well as on the results of hot tensile tests, SEM fracture studies, and electron microprobe element distribution analyses. It must be realized, however, that while all of the test results indicate that successfulcoatings for given substrates can be produced by the ion-plating method used in this work to prepare the coatings, the large number of material combinations which were subjected to the test procedures severely limited the number of repetitions of a given test on a given material combination. In many cases, the quantity of material available for examination when divided between the various tests which were necessary to characterize the effects of the processing on that combination resulted in one test value under given conditions. Although the test results recorded in this report are therefore not statistical averages, every effort was made to cross check the results of different tests to detect anomalous results. Where these were found, efforts were made to determine the accuracy of the result and to correct it if it appeared to be in error. It is believed that the trends indicated by this survey are correct.

ACKNOWLEDGEMENTS

The authors gratefully acknowledge the specific contributions of the following colleagues: K. Taylor, managing the ion plating runs; L. Jackman, scanning electron microscope fracture photographs; J. Knecht and A. Manzione, the electron microprobe analyses; Mrs. A. P. Elkins, making all of the thermal exposures and tensile tests and Mrs. L. A. Jenkins for the manuscript preparation.

REFERENCES

1. D. M. Mattox, J. Vac. Sci. Technol., 10, 47 (1973).

2. S. Aisenberg and R. W. Chabot, J. Vac. Sci. Technol., 10, 104 (1973).

3. D. L. Chamers, D. C. Carmichael and C. T. Wan, Proceedings of the Conference on Sputtering and Ion Plating (NASA Lewis Research Center, 1972) NASA SP-5111. Available from the National Technical Information Service, Springfield, Va. 22151. ($3.00).

4. W. D. Gill and E. Kay, Rev. Sci. Insts., 36, 277 (1965).

5. M. W. Garrett, J. Appl. Phys., 22, 1091 (1951).

APPENDIX

Individual Strength Values Obtained on Fiber Specimens

Material	Dia 10^{-3} in	Dia mm	Breaking Force lbs.	Breaking Force Newtons	UTS kpsi	UTS KN/cm^2	Temp. of Thermal Exposure 24-hr.
W	5.0	.127	8.16	36.6	416	286	25°C
			8.23	36.9	419	289	
			8.22	36.8	419	289	
			8.17	36.6	416	287	
			8.22	36.8	419	289	
			8.22	36.8	419	289	
			8.15	36.5	415	286	
			8.20	36.8	418	288	
			8.22	36.8	419	289	
			8.22	36.8	419	289	
			8.4	37.7	428	295	
			8.38	37.6	427	294	
			8.4	37.7	428	295	
			8.38	37.6	427	294	
Nb	4.8	.122	4.66	20.9	257	177	25°C
			4.60	20.6	254	175	
			4.75	21.3	262	181	
			4.68	21.0	259	178	
			4.66	20.9	257	177	
			4.61	20.7	255	175	
			4.64	20.8	256	177	
			4.65	20.8	257	177	
			4.63	20.8	256	176	
			4.63	20.8	256	176	
	4.85	.123	4.70	21.1	254	175	
			4.66	20.9	257	177	
			4.68	21.0	259	178	
			4.68	21.0	259	178	
NASA Hough Carbon	3.3	.084	2.13	9.55	249	172	
	3.25	.083	1.86	8.34	224	154	25°C
			1.32	5.92	159	110	
			2.05	9.19	247	170	
			1.29	5.78	155	107	
			2.0	8.96	240	165	
			1.05	4.71	127	88	

Material	Dia 10^{-3} in	Dia mm	Breaking Force lbs.	Breaking Force Newtons	UTS kpsi	UTS KN/cm^2	Temp. of Thermal Exposure 24-hr.
Hough Carbon (Cont'd)	3.25	0.83	2.08	9.32	250	172	25°C
			2.0	8.96	240	165	
			1.53	6.86	184	127	
			1.0	4.48	119	82	
			.97	4.34	117	81	
			1.20	5.38	144	99	
Tyco Alumina	12.0	3.05	35.5	159.1	314	216	
			35.8	160.5	317	218	25°C
			35.1	157.3	310	214	
			25.9	116.1	229	158	
			35.0	156.8	309	213	
			37.1	166.3	328	226	
			40.6	182.0	359	247	
			29.0	130.0	256	177	
			21.8	97.7	193	133	
			30.8	138.1	272	188	
	12.2	3.10	54.0	242.0	462	318	
			27.8	124.6	238	164	
			29.0	130.0	248	171	
			20.8	93.2	178	123	
W	5.0	.127	6.9	30.9	352	243	1050°C-1100°C
			6.6	29.6	336	232	
	5.1	.130	6.58	29.5	322	222	
			6.6	29.6	323	223	
Nb	4.8	.122	0.82	3.68	45	31	
			1.15	5.15	64	44	
	5.1	.130	1.22	5.47	60	41	
			1.15	5.15	56	39	
NASA Hough Carbon	3.2	.081	0.65	2.91	81	56	
			1.3	5.83	162	112	
Tyco Alumina	12.0	3.05	21.3	95.5	188	130	
			20.6	92.3	182	125	
	12.35	3.14	30.0	134.5	250	172	
			31.8	142.5	265	183	

Material	Dia 10^{-3}in	Dia mm	Breaking Force lbs.	Breaking Force Newtons	UTS kspi	UTS KN/cm^2	Temp. of Thermal Exposure 24-hr.
W	5.0	.127	6.12	27.4	312	215	1200°C
			1.7	7.6	87	60	
	5.1	.130	6.52	29.2	319	220	
Nb	4.8	.122	1.75	7.84	97	67	
			1.82	8.16	101	70	
	5.1	.130	1.94	8.70	95	65	
NASA Hough Carbon	3.3	.084	0.83	3.72	97	67	
			0.57	2.55	67	46	
Tyco Alumina	12.0	3.05	13.0	58.3	115	79	
			22.4	100.4	198	136	
	12.35	3.14	16.7	74.9	139	96	

Material	Dia 10^{-3} in	mm	Breaking Force lbs	Newtons	UTS kpsi	KN/cm^2	Temp of Thermal Exp. 24 hr.
W/Al_2O_3	5.15	.131	7.05	31.6	338	233	25°C
	5.15	.131	7.2	32.3	346	238	
Y_2O_3	5.65	.144	7.98	35.8	318	219	
	5.25	.133	6.9	30.9	319	220	
TiC	5.4	.137	8.0	35.9	349	240	
	5.2	.132	8.02	35.9	378	260	
	5.2	.132	7.8	35.0	367	253	
	5.3	.135	8.05	36.1	365	251	
WC -14Co	5.25	.133	7.65	34.3	353	243	
	5.2	.132	4.25	19.0	200	138	
ZrC	5.1	.130	6.3	28.2	308	212	
Nb/Al_2O_3	4.85	.123	4.4	19.7	238	164	
Y_2O_3	5.0	.127	4.32	19.4	220	152	
	4.9	.124	1.8	8.07	95	65	
TiC	5.0	.127	4.45	19.9	227	156	
	5.05	.128	4.40	19.7	220	152	
	5.25	.133	4.45	19.9	206	142	
	4.85	.123	4.42	19.8	239	165	
	5.0	.127	4.27	19.1	218	150	
WC-14Co	5.0	.127	4.25	19.0	216	149	
	5.0	.127	4.5	20.2	229	158	
ZrC	4.9	.124	4.35	19.5	231	159	
	5.15	.131	4.1	18.4	197	136	
Hough							
Carbon/Al_2O_3	3.45	.088	2.0	8.96	214	147	
Y_2O_3	3.35	.085	0.7	3.14	79	54	
TiC	3.65	.093	1.65	7.40	158	109	
	3.6	.091	1.65	7.40	162	112	
	3.4	.086	0.9	4.03	99	68	
	3.6	.091	2.22	9.95	218	150	
	3.6	.091	1.22	5.47	120	83	
WC -14Co	3.45	.088	1.35	6.05	144	99	
	3.55	.090	2.0	8.96	202	139	
	3.65	.093	1.86	8.34	178	123	
ZrC	3.5	.089	1.05	4.71	109	75	
	3.35	.085	2.1	9.41	238	164	
	3.75	.095	0.3	1.34	27	19	
	3.6	.091	1.35	6.05	133	92	
	3.6	.091	1.42	6.36	139	96	

Material	Dia 10^{-3} in	mm	Breaking Force lbs	Newtons	UTS kpsi	KN /cm^2	Temp of Thermal Exp. 24 hr.
Tyco							
Alumina/Al_2O_3	12.7	.323	28.0	125.5	221	152	25°C
Y_2O_3	12.3	.312	47.8	214.2	390	269	
TiC	12.6	.320	59.2	265.3	475	327	
	12.45	.316	46.5	208.4	382	263	
	12.3	.312	55.5	248.8	467	322	
	12.5	.292	58.0	260.0	473	226	
	12.3	.312	39.5	177.0	333	229	
WC+14Co	12.5	.292	16.5	74.0	134	92	
	12.35	.314	5.32	23.8	44	30	
ZrC	12.5	.292	40.0	179.3	326	225	
	12.5	.292	45.6	204.4	372	256	

Material	Dia 10^{-3} in	mm	Breaking Force lbs	Newtons	UTS kpsi	KN/cm^2	Temp of Thermal Exp. 24 hr.
W/Al_2O_3	5.15	.131	4.62	20.7	222	153	
	5.15	.131	6.94	31.1	333	229	1000°C
Y_2O_3	5.35	.136	6.38	28.6	284	197	
ZrC	5.1	.130	5.68	25.5	278	191	
Nb/Al_2O_3	4.85	.123	2.79	12.5	151	104	
	4.85	.123	2.88	12.9	156	107	
Y_2O_3	5.1	.127	3.28	14.7	161	111	
ZrC	5.15	.131	3.37	15.1	162	112	
Hough							
Carbon/Al_2O_3	3.45	.088	1.75	7.84	187	129	
Y_2O_3	3.3	.084	1.72	7.71	201	138	
ZrC	3.35	.085	0.92	4.12	105	72	
Tyco							
Alumina/Al_2O_3	12.7	.323	28.5	127.7	225	155	
Y_2O_3	12.3	.312	20.5	91.9	173	119	
ZrC	12.3	.312	41.3	185.1	348	239	
W/Al_2O_3	5.1	.130	4.8	21.5	235	162	1050°-1100°C
Y_2O_3	5.25	.133	6.68	29.9	309	213	
TiC	5.2	.132	1.55	29.4	308	212	
WC-14Co	5.1	.130	5.02	22.5	246	169	
ZrC	5.1	.130	5.7	25.5	279	192	
Nb/Al_2O_3	4.85	.123	2.8	12.6	152	105	
Y_2O_3	5.1	.130	1.66	7.44	81	56	
TiC	Did not survive anneal						
WC-14Co	Did not survive anneal						
ZrC	5.15	.131	3.4	15.2	166	114	
Hough							
Carbon/Al_2O_3	3.45	.088	1.76	7.89	188	130	
Y_2O_3	3.3	.084	1.72	7.71	201	138	
TiC	Did not survive anneal						
WC-14Co	Did not survive anneal						
ZrC	3.35	.085	0.92	4.12	104	72	

Material	Dia 10^{-3}	Dia in mm	Breaking Force lbs	Breaking Force Newtons	Temp of Thermal Exp. 24 hrs.
W/Ni	9.5	.241	8.82	39.5	25°C
Nb/Ni	9.0	.229	5.25	23.5	
Hough Carbon/Ni	8.1	.206	1.75	7.84	
Tyco Alumina/Ni	No data - fiber crumbled in grip				
W/Ni	9.6	.244	5.2	23.3	1050°-1100°C
Nb/Ni	11.5	.292	3.4	15.2	
Hough Carbon/Ni	7.4	.188	1.95	8.74	
Tyco Alumina/Ni	16.0	.406	9.0	40.3	
W/Ni	10.6	.269	3.05	13.7	1200°C
Nb/Ni	No data - fiber crumbled				
Hough Carbon/Ni	7.8	.198	0.67	3.00	
Tyco Alumina/Ni	16.0	.406	11.2	50.2	

Material	Dia 10^{-3} in	mm	Breaking Force lbs	Newtons	Temp. of Thermal Exp. 24 Hrs
W/Al_2O_3/Ni	9.5	.241	8.43	37.8	25°C
Y_2O_3	11.3	.287	8.4	37.7	
TiC	9.6	.244	8.42	37.7	
WC-14Co	10.0	.254	8.1	36.3	
ZrC	9.75	.248	8.44	37.8	
Nb/Al_2O_3/Ni	7.4	.188	4.52	20.3	
Y_2O_3	9.8	.249	4.58	20.5	
TiC	9.8	.249	4.53	20.3	
WC-14Co	10.2	.259	4.45	19.9	
ZrC	10.7	.272	4.47	20.0	
Hough					
Carbon/Al_2O_3/Ni	No fiber available				
Y_2O_3	Did not coat				
TiC	7.7	.196	1.5	6.72	
WC-14Co	9.25	.235	2.32	10.4	
ZrC	7.7	.196	2.12	9.50	
Tyco					
Alumina/Al_2O_3/Ni	Deleted				
Y_2O_3	16.4	.417	4.41	19.8	
TiC	16.4	.417	30.2	135.4	
WC-14Co	18.0	.457	4.47	20.0	
ZrC	18.6	.472	0.92	4.12	
W/Al_2O_3/Ni	9.5	.241	0.69	3.09	1050°-1100°C
Y_2O_3	11.3	.286	5.8	26.0	
TiC	9.6	.244	2.71	12.1	
WC-14Co	10.0	.254	0.43	1.93	
ZrC	9.75	.248	2.5	11.2	
Nb/Al_2O_3/Ni	7.4	.188	5.78	25.9	
Y_2O_3	9.6	.244	0.37	1.66	
TiC	9.8	.249	3.68	16.5	
WC-14Co	10.2	.259	6.25	28.0	
ZrC	10.7	.272	6.8	30.5	
Hough					
Carbon/Al_2O_3/Ni	9.35	.237	3.5	15.7	
Y_2O_3	Fiber did not coat				
TiC	No data				
WC-14Co	9.25	.235	0.52	2.33	
ZrC	7.7	.196	1.74	7.80	

Material	Dia 10^{-3} in	mm	Breaking Force lbs	Newtons	Temp. of Thermal Exp. 24 Hrs
Tyco					
Alumina/Al_2O_3/Ni	Deleted				1050°-1100°C
Y_2O_3	16.4	.417	11.2	50.2	
TiC	16.4	.417	5.45	24.4	
WC-14Co	18.0	.457	9.7	43.5	
ZrC	18.6	.472	16.8	75.3	
W/Al_2O_3/Ni	9.5	.241	4.35	19.5	1200°C
Y_2O_3	11.3	.286	4.21	18.9	
TiC	9.6	.244	5.4	24.3	
WC-14Co	10.0	.254	6.1	27.3	
ZrC	9.75	.248	1.92	8.61	
Nb/Al_2O_3/Ni	7.4	.188	4.25	19.0	
Y_2O_3	9.6	.244	4.72	21.2	
TiC	9.8	.249	4.15	18.6	
WC-14Co	10.2	.259	3.66	16.4	
ZrC	10.7	.272	4.35	19.5	
Hough					
Carbon/Al_2O_3/Ni	No test				
Y_2O_3	Fiber did not coat				
TiC	No data*				
WC-14Co	No data				
ZrC	No data				
Tyco					
Alumina/Al_2O_3/Ni	Deleted				
Y_2O_3	16.4	.417	12.2	54.7	
TiC	16.4	.417	22.0	98.6	
WC-14Co	18.0	.457	45.2	202.6	
ZrC	18.6	.472	11.25	50.4	

*fiber adhered to holder during anneal

Material	Dia 10^{-3} in	mm	Breaking Force lbs	Newtons	Temp. of Thermal Exp. 24 hrs
W/Al_2O_3/Ti	7.55	.192	8.4	37.7	25°C
Y_2O_3	No test				
TiC	7.6	.193	11.60	52.0	
WC-14Co	9.9	.251	16.65	74.6	
ZrC	10.3	.262	18.0	80.7	
Nb/Al_2O_3/Ti	8.0	.203	8.5	38.1	
Y_2O_3	No test				
TiC	8.0	.203	7.0	31.4	
WC-14Co	7.6	.193	7.8	35.0	
ZrC	---	---			
Hough					
Carbon/Al_2O_3/Ti	No test				
Y_2O_3	No test				
TiC	6.65	.169	2.95	12.3	
WC-14Co	No test				
ZrC	5.95	.151	2.4	10.8	
Tyco					
Alumina/Al_2O_3/Ti	Deleted				
Y_2O_3	14.3	.363	24.3	108.9	
TiC	14.55	.370	32.5	145.7	
WC-14Co	13.6	.345	44.0	197.2	
ZrC	16.25	.413	17.0	76.2	
W/Al_2O_3/Ti	7.55	.192	7.63	34.2	870°C
Y_2O_3	No test				
TiC	7.6	.193	8.92	40.0	
WC-14Co	9.9	.251	7.60	34.1	
ZrC	10.3	.262	7.55	33.8	
Nb/Al_2O_3/Ti	8.0	.203	3.56	16.0	
Y_2O_3	No test				
TiC	8.0	.203	4.60	20.6	
WC-14Co	7.6	.193	5.02	22.5	
ZrC	---	---			

Material	Dia 10^{-3} in	mm	Breaking Force lbs	Newtons	Temp. of Thermal Exp. 24 hrs
Hough					
Carbon/Al_2O_3/Ti	No test				870°C
Y_2O_3	No test				
TiC	No data - fiber crumbled				
WC-14Co	No test				
ZrC	Did not survive				
Tyco					
Alumina/Al_2O_3/Ti	Deleted				
Y_2O_3	14.3	.363	18.7	83.8	
TiC	14.55	.370	16.5	74.0	
WC-14Co	13.6	.345	15.2	68.1	
ZrC	16.25	.413	19.5	87.4	